Biogenic aerosol precursors in decaying Antarctic sea ice and brines in late summer

Odile Crabeck[1*], Arianna Rocchi[2,3*], C. Wohl[2,4,5], M. F. Fitzsimons[6], P. Akenga[6], A. Sotomayor[7], M. Vila[2], D. Vaqué[2], E. L. Sà[2], B. Delille[1], S. Muller[1,8], Y. M. Castillo[2], T. Barthelmeß[9], A. Engel[9], M. Dall'Osto[2], E. Berdalet[2] and R. Simó[2] .

[1]Chemical Oceanography Unit, Science Faculty, University of Liège, Liège, Belgium
[2]Institute of Marine Sciences (ICM-CSIC), Department of Marine Biology and Oceanography, Barcelona, Spain.
[3]University of Barcelona, Faculty of Earth Sciences, Barcelona, Spain.
[4]Centre of Ocean and Atmospheric Sciences, School of Environmental Sciences, University of East Anglia, Norwich, UK.
[5]National Centre for Atmospheric Science, University of East Anglia, Norwich, UK.
[6]University of Plymouth, Biogeochemistry Research Centre, School of Geography, Earth and Environmental Sciences, Plymouth, UK.
[7]Marine Technology Unit (UTM-CSIC), Barcelona, Spain.
[8]Department of Geosciences, Environment and Society, Université Libre de Bruxelles, Brussels, Belgium.
[9]GEOMAR Helmhotz Centre for Ocean Research Kiel, Kiel, Germany.

*First authors ocrabeck@uliege.be ORCID 0000-0003-1882-9303, rocchi@icm.csic.es ORCID 0000-0002-1193-2562

Corresponding authors: ocrabeck@uliege.be, rsimo@icm.csic.es

ABSTRACT

Alkylamines, methanethiol (MeSH), and a suite of volatile organic compounds (VOCs) concentrations are reported for the first time from decaying Antarctic sea ice, alongside sulfur compound concentrations (dimethylsulfoniopropionate, DMSP) and dimethylsulfide (DMS)). Measurements from different sea ice depths and brines were compared with the surrounding surface seawater in the northern Weddell Sea. Dissolved trimethylamine (TMA), dimethylamine (DMA), and diethylamine (DEA), as well as particulate trimethylamine, were detected in nearly all samples, while monomethylamine (MMA) consistently remained below the detection limit. Trimethylamine (dissolved + particulate) was particularly enriched in bottom sea ice (average: 902.4 ± 989.1 nM, n = 3) compared to seawater (median: 43.9 nM, n = 5). MeSH also showed enrichment in bottom sea ice (median 0.7 nM, n = 5) compared to seawater (median 0.3 nM, n = 5). Its vertical distribution

within sea ice aligned with the distribution of Chlorophyll-a (Chl-a), and other sulfur compounds, all peaking in the sea ice bottom. Target VOCs showed highest median concentrations in sea ice (48.3 nM acetone, 0.9 nM isoprene, 0.3 nM benzene, 1.0 nM toluene and 0.6 nM xylene, n = 16) compared to seawater, with concentrations increasing towards the sea ice-atmosphere interface. These results confirm that sea ice is a hotspot for alkylamines, sulfur-containing compounds, and other VOCs, even during the advanced stages of sea ice decay, which are also periods of survival/resting cyst formation. The data also suggest that these compounds are probably associated with biofilms on the ice walls rather than freely dissolved in brines. These findings highlight that sea ice acts as a dynamic biogeochemical interface, rich in biogenic aerosol precursors sourced from ice microbiota, with important implications for polar atmospheric chemistry and climate-relevant processes.

1. INTRODUCTION

As a central component of the Southern Ocean system, sea ice strongly influences climate through its effects on albedo, gas exchange, and ocean–ice–atmosphere interactions. Structured as a matrix of ice crystals permeated by a complex network of brine channels and pores (Underwood et al., 2010), sea ice also serves as a habitat, hosting diverse sympagic (ice-related) microbial communities (Vancoppenolle et al., 2013; van Leeuwe et al., 2018; Rocchi et al., 2022). As sea ice melts through summer, it enters a phase known as decaying sea ice, characterized by thinning, increased light availability and permeability, melt-driven changes in salinity, and shifts in microbial communities. These communities originate from surface planktonic assemblages and are dominated by phototrophic taxa such as diatoms, dinoflagellates, and haptophytes, alongside heterotrophic and mixotrophic organisms (Thomas et al., 2010; Wilkins et al., 2013; van Leeuwe et al., 2022). The composition of these assemblages varies seasonally, with shifts between diatom- and dinoflagellate-dominated communities and certain protists overwintering as cysts (Garrison and Close, 1993; Stoecker et al., 1997; Piquet et al., 2008).

Recent works (Dall'Osto et al., 2017; Dall'Osto et al., 2022; Willis et al., 2023) highlighted that sea ice biota can play a key role in aerosol loading over polar oceans, influencing cloud coverage and, hence, providing feedback on climate. The algal organic solute dimethylsulfoniopropionate (DMSP) reaches its highest global concentrations in polar regions (Galí et al., 2015) and is several orders of

magnitude more concentrated in sea ice than in seawater, where microalgae use it as a cryoprotectant osmolyte to survive extreme freezing conditions (Trevena and Jones, 2006; Tison et al., 2010; Damm et al., 2016; Hopkins et al., 2023; Burke et al., 2024). Its breakdown product, dimethylsulfide (DMS), is the primary form of marine volatile methylated sulfur (VMS) emissions, contributing to aerosol formation and climate feedback mechanisms (Simó, 2001; Stefels et al., 2007; Tison et al., 2010). Similar to DMS but less known, methanethiol (MeSH), is also a DMSP degradation product (Kiene, 1996; Stefels et al., 2007). Recent studies reported high concentrations of MeSH in polar waters (Kiene et al., 2021; Gros et al., 2023; Mynard et al., 2025) with a significant contribution to atmospheric aerosol load (Wohl et al., 2024). Indeed, metagenomic analysis revealed that the enzymatic machinery for MeSH production is widespread in polar plankton (Teng et al., 2021). However, to our best knowledge, MeSH measurements in sea ice are entirely lacking.

Complementing sulfur compounds, alkylamines also play a role in primary and secondary aerosol formation, with consequences for new particle formation, aerosol growth, and cloud condensation nuclei numbers (Dall'Osto et al., 2017; 2019; Brean et al., 2021; Liu et al., 2022; Corral et al., 2022). Recent studies in polar environments observed elevated concentrations of alkylamines and nitrogen (N)-containing osmolytes in marine and atmospheric samples near sea ice, suggesting that sea ice microbiota could contribute significantly to organic N emissions (Dall'Osto et al., 2017; Rinaldi et al., 2020; Rocchi et al., 2025). Similar to DMSP, alkylamines are metabolized by phytoplankton and bacteria as a source of energy, while their N-precursors function as osmolytes (Fitzsimons et al., 2024; Rocchi et al., 2025). Some correlation between alkylamines and DMSP has recently been observed in Antarctic waters (Rocchi et al., 2025), suggesting links between the oceanic N- and S- cycles in polar environments. However, the presence and distribution of alkylamines within sea ice and brines remain poorly understood and largely unexplored.

In addition to N- and S- volatiles, isoprene and acetone have been detected in polar oceans, where they are thought to impact atmospheric chemistry (Wohl et al., 2020; 2022; Zhou et al., 2022). Isoprene, an aerosol-forming biogenic VOC, is widely produced by phytoplankton and actively cycled within microbial food webs (Shaw et al., 2010; Wohl et al., 2020; Simó et al., 2022). In addition, acetone is an oxygenated VOC that affects the oxidative capacity of the marine atmosphere. It is produced predominantly from the photochemical degradation of dissolved organic

matter, with phytoplankton providing an additional source (Halsey et al., 2017; Schlundt et al., 2017; Davie-Martin et al., 2020) and microbial uptake constituting its main sink in seawater (Heald et al., 2008; Dixon et al., 2013; 2014). BTX compounds (benzene, toluene, and xylene), which influence hydroxyl radical concentrations and secondary aerosol formation (Wohl et al., 2023b), are traditionally considered anthropogenic pollutants. However, growing evidence from cultured marine microorganisms (Romoli et al., 2011; Misztal et al., 2015; Omori et al., 2025; Padaki et al., 2025) and field observations in the Southern Ocean (Rocco et al., 2021; Wohl et al., 2023b) demonstrates biological production pathways. While sea ice biota have the potential to actively produce and recycle isoprene, acetone, and BTX compounds, their distribution and concentration in sea ice remain unexplored to date.

This study investigates the presence and distribution of the aforementioned biogenic volatiles and aerosol precursors in Antarctic sea ice and brines during late summer. While our survey was limited to a few ice stations in March 2023 in the Weddell Sea, we report the first comprehensive quantifications of dissolved and particulate alkylamines, MeSH, acetone, isoprene, and BTX compounds. These novel observations are complemented by an extensive suite of biogeochemical and physical measurements. Given the ecological significance of sea ice biomes and the influence of S- and N-containing volatiles and other VOCs on present and future aerosol loads, advancing our understanding of their distribution in sympagic environments is of primary importance for improving predictions of biogeochemical feedbacks on climate. Due to the non-linear responses of clouds to aerosols, better quantification of aerosol precursors from sea ice can help close the gap between the observed and the modelled radiative budget in the Southern Ocean (McCoy et al., 2015; Fiddes et al., 2022; Fung et al., 2022; Mallet et al., 2023; Wohl et al., 2024). Our study also provides a description of the biogeochemical properties of decaying sea ice and brines in late summer, a time of the year currently under-represented in data collations (Fripiat et al., 2017; Meiners et al., 2018; Dalman et al., 2025).

2. Materials and methods

Study area and sampling strategy. The PolarChange (Aerosol Emissions in Changing Polar Environments) expedition was conducted aboard the RV *Hesperides* around the Antarctic Peninsula in the Southern Ocean from 14 February to 17 March 2023, during the late austral summer. The

survey took place long after the spring algal bloom. In the Weddell Sea, we encountered a strip of drifting sea ice floes (Figure S1) that we sampled four times between March 2 and 5. At each ice station, up to four replicate ice cores were extracted using an ice corer with an internal diameter of 9 cm (Kovacs Ent., Lebanon, USA). In situ sea ice temperature was measured on the first ice core with a depth resolution of 5 cm at the top and bottom, and 10 cm in the internal part using a calibrated probe (Testo 720) inserted into predrilled holes (with the same diameter as the probe) perpendicular to the ice core axis. The precision of the probe was ± 0.1°C. This "temperature" ice core was immediately cut into 5 cm slices, stored in polyethylene buckets, and left to melt. Back in the onboard laboratory, bulk ice salinity was measured with a portable conductivity meter (WTW Cond 3110 conductometer) with a precision of ± 0.1.

In sea ice, the distinction between bulk and brine chemical concentrations is an important concept. Bulk concentration refers to the chemical concentration of melted ice (usually expressed in units per liter of meltwater) and includes the meltwater from the ice matrix, the liquid fraction from the brine and the material that was initially in the brine or sticking on the ice walls. In contrast, the brine concentration refers to the chemical concentration within the brine itself and is expressed in units per liter of brine.

For biogeochemical compounds in bulk ice, 10 cm sections at the top, bottom and middle part of the ice cores were immediately cut in situ, placed in polyethylene bags and stored in an insulated box filled with individual cooling bags before being brought to the ship laboratory. Once on board, sections for biological analyses (Chl-a, bacteria, virus and microplankton; processing details are indicated in the next section) were left to melt in acid-cleaned plastic buckets together with known volumes of filtered seawater (filter pore size of 0.22 μm) collected on the same day near the sea ice floes. The resulting concentrations were corrected considering the respective dilution factors. Other ice core sections were left to melt without the addition of filtered seawater for the analyses of nutrients, alkylamines, sulfur compounds, VOCs, particulate organic carbon and nitrogen (POC and PON) concentrations. Among these, the sections for DMS, MeSH and VOC analysis were placed in an airtight vacuum-sealed polytetrafluoroethylene (PTFE) bag and left to melt in the dark. Note that alkylamines were collected only in the top and bottom sections of the sea ice cores.

Brines were collected in situ using the sackhole technique, which involves drilling a hole through the ice to a desired depth and allowing brines from the surrounding ice to drain into the hole (Miller et al., 2015). Sackholes were drilled from the ice floe surface down to 15, 50, and 95 cm depth, to allow gravity-driven brine collection. Each sackhole remained covered with a plastic lid to minimize atmospheric contamination. Brines were collected using a portable peristaltic pump (Master Flex®, E/S portable sampler) 15 to 30 min after drilling, depending on how quickly the brine drained into the hole. Aliquots for determination of Chl-a, bacteria, virus and nanoplankton (n = 14) and microplankton composition (n = 8) and nutrient analyses (n = 11) were processed as indicated in the next section. For alkylamines (n = 8) sulfur compounds (n = 15) and VOCs (n = 15) subsamples were collected in a gas-sensitive fashion (i.e., no bubbles) into 50 mL and 250 mL glass bottles with glass caps kept in the dark until filtration and conditioning for storage for alkylamine and immediate analysis on board for VOCs, DMS(P), MeSH, respectively.

Seawater samples (n = 5) were hand-collected off the front of the Zodiac in 500 mL glass bottles during ice sampling stations. To remove large particulates and organisms, the seawater samples were prefiltered using a 200 μm mesh filter, before filtration or preservation for Chl-a, bacteria, viruses and nano- and microplankton determination. Seawater samples for alkylamine, sulfur compounds, and VOC analyses were collected without 200 μm prefiltration in a gas-sensitive manner to avoid the artificial release of these compounds during manipulation.

Alkylamine analysis protocol: concentrations of trimethylamine (TMA), dimethylamine (DMA), diethylamine (DEA), and monomethylamine (MMA). Seawater, melted sea ice and brine samples were collected into 50 mL tubes and filtered through a 47 mm GF/F filter (0.7 μm pore size) by gravity (~60 min). The filtered sample was then collected into another 50 mL tube containing 1% concentrated hydrochloric acid and stored at 4°C in the refrigerator for further analysis of dissolved amines. GF/F filters were placed in 2 mL Eppendorf tubes and stored at -80°C for particulate amine analysis. All determinations were performed ~6 months after collection. For dissolved alkylamine analysis in seawater, we followed the optimised method described by Akenga and Fitzsimons (2024), which uses an automated online headspace-based solid-phase microextraction (HS-SPME) followed by gas chromatography with nitrogen-phosphorus detection (GC-NPD). MMA, DMA, TMA, and DEA standard solutions were prepared in hydrochloride form. Stock solutions were acidified, and calibration solutions were prepared. Aliquots were saturated

with NaCl, adjusted to pH >13.0 with NaOH, and sealed. Cyclopropylamine (CPA) was used as an internal standard. For particulate alkylamine analysis, filters were defrosted, treated with NaOH (10 M), and run similarly to dissolved amine forms (Rocchi et al., 2025). The resulting volatile analytes were extracted onto an SPME fibre, injected into the GC system, thermally desorbed, separated, and measured.

Total dimethylsulfoniopropionate (DMSP) concentrations. Seawater, sea ice and brine samples for total DMSP (DMSPt) analysis were collected into ~30 mL borosilicate serum vials and processed according to Kinsey and Kieber (2016). The vials were uncapped and individually heated in a microwave until the formation of the first boiling bubble, at which point heating was stopped. After cooling, 30 µL of 37% HCl was added to each vial to remove DMS and preserve DMSP. Acidified samples were stored at room temperature in the dark. Within 6 months of collection, DMSP was hydrolyzed to DMS via alkaline treatment with NaOH for at least 24 hours. The released DMS was quantified using a cryogenic purge-and-trap system coupled to a Thermo Fisher TRACE 1300 gas chromatograph with flame photometric detection, following the method of Masdeu-Navarro et al. (2022).

Volatile organic compound (VOC) concentrations VOCs were measured using a segmented flow coil equilibrator (SFCE) (Wohl et al., 2019) coupled to a Vocus proton transfer reaction time of flight mass spectrometer (PTR-ToF-MS; Tofwerk, Switzerland, and Aerodyne Research, USA). The water was withdrawn into the SFCE from the bottom of the glass bottles of brine, seawater or the PTFE bag containing melted sea ice. Dissolved VOC concentrations were calculated as described previously by Wohl et al. (2023b) for benzene and toluene, Wohl et al. (2024) for DMS and MeSH and Wohl et al. (2022) for acetone and isoprene. Dissolved xylene concentrations were calculated using the solubility recommended by Staudinger and Roberts (2001), as listed in Sander (2023). We note that fragments of various compounds, including long-chain aldehydes and cycloalkanes, have been observed to contribute to the $C_5H_8H^+$ ion (Jensen et al., 2023; Coggon et al., 2024), which is attributed to isoprene in this study. This interference has been predominantly observed in polluted urban air (Pfannerstill et al., 2024) or indoor air (Ditto et al., 2024). Many of these interfering compounds are somewhat insoluble in seawater suggesting the amount in equilibrator headspace air is likely small (see Sander, 2023); for example, nonanal and isoprene have somewhat similar solubilities. Unfortunately, we could not determine the contribution of fragments to $C_5H_8H^+$ in this

measurement. Hence, the concentrations of isoprene reported here are an upper limit estimate of the true dissolved concentration. We did observe other nonanal ions in our spectra (i.e. *m*/*z* 111.117 and *m*/*z* 125.132 (Pfannerstill et al., 2024)), though these signals were small and poorly correlated with $C_5H_8H^+$, suggesting a relatively small interference. Overall, we cautiously estimate the systematic uncertainty of our measurements to be 20% for DMS, 50% for MeSH, 50% for the BTX compounds, 20% for acetone, and 50% for isoprene. The uncertainty here is significantly larger because sampling and handling have the potential to alter VOC concentrations (e.g., bacterial degradation, atmospheric contamination), which we cannot quantify. Because the systematic uncertainty affects all measurements in the same way and the measurement noise for these compounds is much smaller (typically 5–10%), our analysis and interpretation focus on relative differences between sea ice layers, seawater, and brines, even though absolute concentrations are somewhat uncertain.

Chlorophyll-a. Chl-a concentration was measured fluorometrically following Yentsch and Menzel (1963). Water samples (seawater, bulk ice melt water, and brine) (200–750 mL) were filtered onto 25 mm Whatman GF/F glass fibre filters, which were immediately frozen at -20°C for preservation. Onboard analyses were conducted within a few days, with filters extracted in 6 mL of 90% acetone at 4°C in the dark for 24 hours to ensure passive pigment release. Fluorescence readings of the extracts were performed using a Turner 10AU fluorometer, calibrated with a spinach-derived chlorophyll standard (Sigma C5357) and verified with a Becton-Dickinson spectrophotometer.

Viral and bacterial abundance. To estimate viral and bacterial abundances, 2 mL of water samples were preserved using specific fixatives: glutaraldehyde (0.5% final concentration) for viral counts and 1% paraformaldehyde plus 0.05% glutaraldehyde for bacterial abundance analyses. Fixed samples were incubated in the dark at 4°C for 15–30 min, flash-frozen in liquid nitrogen, and stored at -80°C following Brussaard (2004) and Gasol and Del Giorgio (2000). Analyses were conducted up to 5 months later using a Cytoflex flow cytometer for viral counts and Cyflow Cube 8 for bacterial abundance at the Institute of Marine Sciences, ICM-CSIC laboratory. For viral counts, samples were diluted with TE (Tris–EDTA) buffer (10 mM Tris:1 mM EDTA, Ethylenediaminetetraacetic acid), stained with SYBR Green I (50x, final 1%), heated in an 80°C water bath for 10 min, and processed at a flow rate of 60 μL min^{-1} according to Brussaard (2004). Viruses were identified on bivariate scatter plots of green fluorescence (stained nucleic acids) versus

side scatter (SSC). Water samples for bacterial counts were stained with SYBR Green I (50x, final concentration 1%) and incubated in the dark for 5 min. Bacteria were detected using a 488 nm laser, with populations differentiated based on side scatter (SSC) versus green fluorescence (FL1).

Nano- and microplankton abundance and composition. Samples for the enumeration of nanophytoplankton (2–20 μm) were collected in 5 mL cryovials, fixed with 1% glutaraldehyde, and immediately frozen in liquid nitrogen, following the protocol of Vaulot et al. (1989). Samples were analysed at the ICM-CSIC laboratory, where cells were counted using a CyFlow Cube 8 flow cytometer (FC; Sysmex) equipped with a 488 nm laser for phytoplankton detection. Red fluorescence vs side scatter plots allowed counts of nanophytoplankton, among which cryptophytes were identified by their complementary orange fluorescence. Additionally, the microplankton community was analysed using the Utermöhl method on Lugol's iodine-preserved samples and examined under an inverted microscope following the procedure of Edler and Elbrächter (2010). Phytoplankton were categorised by the taxonomic groups, including dinoflagellates and their cysts, diatoms, and microzooplankton ciliates. Whenever possible, organisms were identified to the genus or species level. More information is provided in Rocchi et al. (2025).

Particulate organic carbon and nitrogen. POC and PON in water samples (i.e., seawater, bulk ice melt water and brine) were measured by filtering 250–1000 mL samples onto pre-combusted (450°C, 4 hours) 25 mm GF/F glass fibre filters (Whatman) under low pressure (<20 mm Hg). Filters were stored at -80°C until analysis. Before analysis, filters were air-dried at room temperature and exposed to 37% HCl vapour in a sealed chamber to remove inorganic carbonates, while inorganic nitrogen was assumed to be negligible. POC and PON content were then determined using a Perkin-Elmer 2400 CHN Elemental Analyzer at the Scientific and Technical Services of the University of Barcelona. In this study, POC and PON are used as proxies for particulate organic matter, encompassing both living and non-living material, such as cells, extracellular compounds, and detritus containing organic C and N.

Dissolved inorganic nutrient analysis. To measure nutrient concentrations, water (i.e., seawater, melted bulk ice and brine) was collected into a 50 mL polypropylene tube, designated for inorganic nutrients (nitrate, nitrite, ammonium, phosphate, and silicate). Samples were frozen immediately

after collection and stored at -20°C until analysis. Inorganic nutrients were quantified using a high-resolution AA3 HR autoanalyzer (Seal Analytical) at the ICM-CSIC Chemical Service.

Transparent exopolymer particles (TEP). Melted ice core and brine samples were filtered in triplicate onto polycarbonate filters (25 mm, 0.45 µm pore size, Nucleopore, Whatman) in volumes ranging from 30 to 70 mL. The reference seawater samples were processed in the same manner, but 100 mL volumes were filtered. For operational blanks, 10 mL of MilliQ water was filtered. The filters were stained with an acidic Alcian Blue solution (0.02%, pH 2.5). Filters were folded, transferred to Eppendorf tubes, frozen, and stored at -20°C until analysis in the ICM-CSIC laboratory. The TEP concentration was determined colorimetrically. Filters were transferred into 15 mL tubes, 6 mL of sulfuric acid (80%) was added, and the tubes were incubated for two hours. The absorption of the amount of Alcian Blue, equivalent to the resolved TEP, was determined against MilliQ at a wavelength of 787 nm. The TEP concentration was calibrated against a standard, the polysaccharide xanthan gum (XG), and is expressed in XG equivalents (µg $L^{-1)}$. The mean value of the associated operational blanks was subtracted from the samples. If the relative standard deviation was larger than 35%, the deviating triplicate was removed. TEP was measured following the protocol of Engel (2009).

3. Results and Discussion

3.1 Sea ice physical state

Sea ice temperature and salinity vary strongly through growth and decay. While ice exhibits a strong negative temperature gradient during growth, warming from increased radiation throughout spring and summer leads to an isothermal profile. At the four ice stations, the sea ice was about 1 meter thick and warm with an isothermal ($\bar{x}$ = -1.45 ± 0.15°C) temperature profile typical of decaying summer sea ice (Figure 1A). During initial ice formation in autumn and early winter, bulk salinities can range between 5 and 15, depending on growth rate and temperature (Petrich and Eicken, 2010). As winter progresses and ice thickens, brine rejection reduces the bulk salinity, especially in the internal layers, producing a typical C-shaped profile. In spring and summer, surface warming triggers internal melting, diluting brine pockets and leading to episodic flushing events (Notz and Worster, 2009). During these events, meltwater percolates through the ice matrix, mobilizing and expelling brine, which further reduces the bulk salinity of the ice column closer to

freshwater conditions. Consequently, the ice at the four ice stations was depleted in salinity. Bulk ice salinity was always below 2, except for the very bottom and top layers, and the brine salinity was at all times lower than seawater salinity (Figure 1B, C), implying that the brine was diluted by internal melting. A low salinity and an isothermal temperature profile are characteristic of old summer rotten sea ice partially washed out of its solutes. The seasonal decline in bulk salinity has critical implications for sea ice structure and permeability, as well as for its role as a habitat and medium for biogeochemical processes.

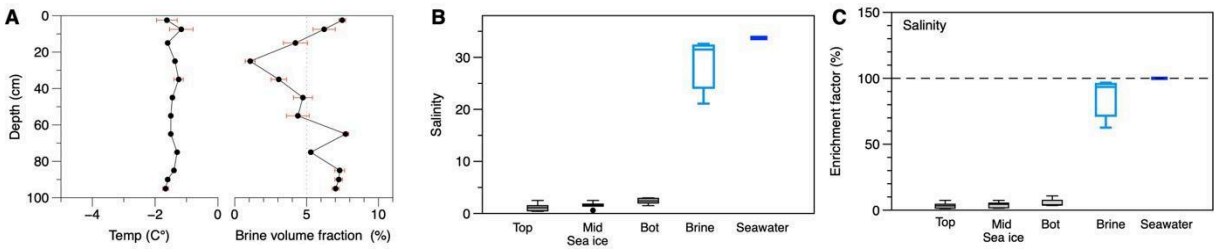

Figure 1. Sea ice physical properties. Temperature in (°C) and brine volume fraction (%) profiles in the sea ice cores **(A)**. IQR box plots of the salinity **(B)** and enrichment factor (%) **(C)** for the top (n = 5), middle (Mid, n = 6) and bottom (Bot, n = 5) ice layers, brine (n = 12) and seawater (n = 5). Box plots show the interquartile range (IQR; 25th–75th percentile), with the horizontal line indicating the median and whiskers extending to 1.5 × IQR.

During the survey, the brine volume fraction in some internal ice layers (20–60 cm depth) fell below the 5% permeability threshold (Golden, 2003), indicating that the brine channels in these layers were likely disconnected and that the upper ice was not effectively linked to the underlying seawater (Figure 1A). Convective processes implying the rejection of dense salty brine and its replacement by less dense and less salty underlying seawater were also clearly limited given that the brine displays a stable density profile implying a strong stratification.

The concentrations of compounds within sea ice can be influenced by biological as well as physical processes. Salinity is used as a reference to evaluate the significance of biological changes in sea ice solute concentrations, as physical processes solely influence salinity. A solute is considered conservative against salinity if its chemical concentration is proportional to salinity. Deviations from this relationship generally stem from biological or chemical processes occurring within sea ice. In order to evaluate the importance of biogeochemical processes in shaping the distribution and

concentration of components (Chl-a, POC and PON, microorganisms, nutrients, alkylamines, S-compounds and VOCs), we used the enrichment factor, defined as $EF_{ice/brine} = C_{ice/brine} / C_{sw} \times 100$ where C is the concentration of a given component in ice (C_{ice}) or brine (C_{brine}) and seawater (C_{sw}) (Table S1). This enrichment factor allows (1) to evaluate how a component is enriched in sea ice or brine compared to seawater, and (2) how its concentration deviates from salinity. A difference in the enrichment factor to the salinity enrichment factor implies that biogeochemical processes are involved.

3.2 Sea ice biogeochemical and microbiological state

Concentrations of Chl-a, POC, PON, viruses, bacteria, and relative abundance of cryptophytes, dinoflagellates, diatoms, and ciliates (Figure 2), as well as nutrients distribution (Figure 3), enable the characterization of the biogeochemical state of sea ice (Figures 1–3).

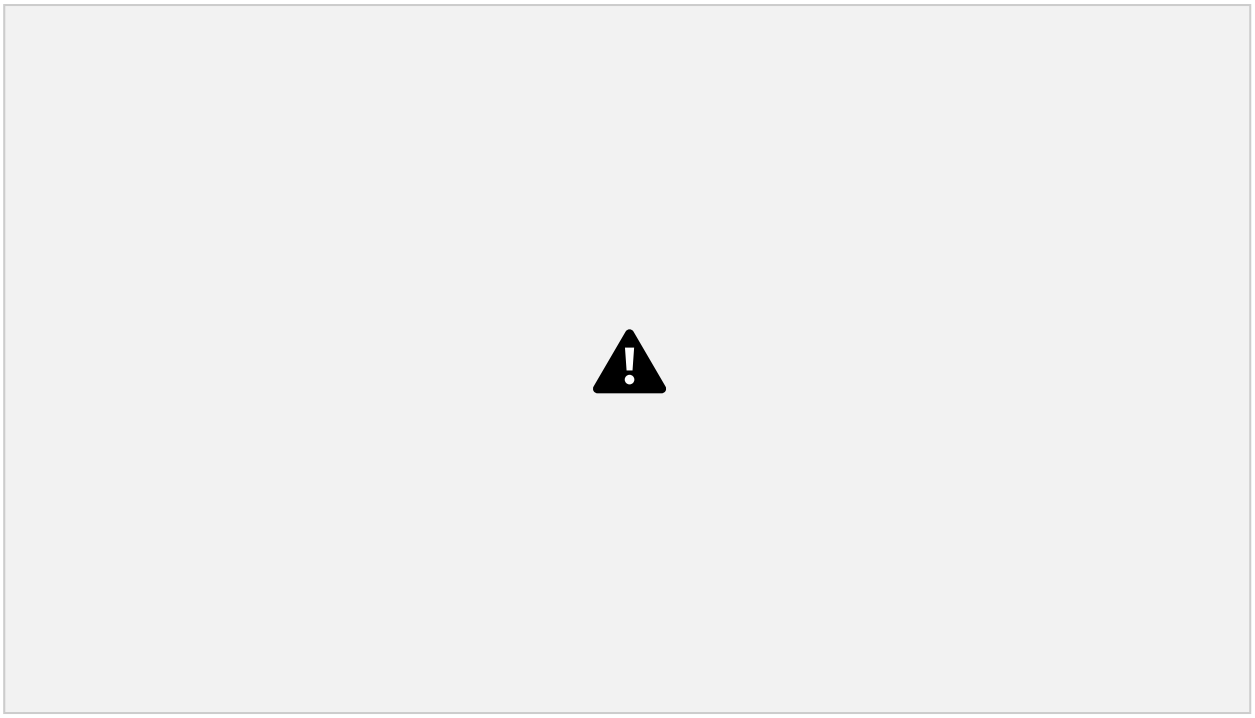

Figure 2. Biological properties of the sea ice, brines and seawater. IQR box plot of the concentration and enrichment factor of the following parameters: Chl-a **(A and C)**, POC **(B and C)**, PON **(B and C)**; virus **(D and F)** and bacterial (**E and F)**, TEP **(G)**, for the top, middle (Mid) and bottom (Bot) ice layers, brine and seawater. The abundances of the main microplankton groups

(diatoms, dinoflagellates and ciliates) expressed as % of the total cell numbers in **(K)**. Box plots show the interquartile range (IQR; 25th–75th percentile), with the horizontal line indicating the median and whiskers extending to 1.5 × IQR. The number of data points for each box plot is reported in Table 1.

Table 1. Biological and biogeochemical variables in sea ice, brine and seawater Columns depict the average ± standard deviation, the median and 25th-75th percentiles (IQR) of the concentrations or abundances, and the sample number (n) in top, middle (Mid) and bottom (Bot) layers of sea ice, as well as in brines and seawater (SW).

Sample	Chl-a (μg L^{-1})				POC (μM)				PON (μM)			
	avg ± SD	median	IQR	n	avg ± SD	median	IQR	n	avg ± SD	median	IQR	n
Top	0.17 ± 0.10	0.13	0.10-0.22	3		22.3		1		0.8		1
Mid	0.31 ± 0.14	0.4	0.26-0.41	3		36.8		1		1.8		1
Bot	1.00 ± 0.61	0.92	0.61-1.35	3		47		1		2.1		1
Brine	0.31 ± 0.26	0.21	0.16-0.30	14	23.8 ± 9.6	22.5	17.6-29.3	3	1.8 ± 0.2	1.9	1.7-2.0	3
SW	0.18 ± 0.03	0.17	0.16-0.19	5	5.4 ± 2.4	4.9	4.3-7.2	4	0.7 ± 0.3	0.6	0.5-0.9	4
Sample	Virus (10^6 viruses mL^{-1})				Bacteria (10^5 cells mL^{-1})				TEP (µg Xeq L^{-1})			
	avg ± SD	median	IQR	n	avg ± SD	median	IQR	n	avg ± SD	median	IQR	n
Top	14.9 ± 14.3	5.3	4.86-20.2	3	5.4 ± 6.0	1.2	1.1-7.6	3	113.6 ± 5.7	44.3	36.4-158.8	3
Mid	39.3 ± 7.5	41.4	35.3-44.4	3	5.0 ± 3.7	2.9	2.4-6.6	3	198.8 ± 11.2	177.2	158.1-224.3	3
Bot	55.8 ± 15.0	62.6	48.8-66.2	3	5.4 ± 3.0	3.6	3.2-6.6	3	223.5 ± 34.1	143.6	179.8-250.8	3
Brine	6.3 ± 2.4	5.5	4.2-4.5	14	4.6 ± 2.7	3	2.5-5.8	14	92.6 ± 6.2	84.5	67.0-112.3	8
SW	3.1 ± 0.7	2.9	2.7-2.9	5	2.4 ± 0.4	2	2.0-2.3	5	48.7 ± 2.8	47	44.3-53.1	4
Sample	Nitrate+Nitrite (μM)				Silicate (μM)				Phosphate (μM)			
	avg ± SD	median	IQR	n	avg ± SD	median	IQR	n	avg ± SD	median	IQR	n
Top	3.1 ± 1.5	3.6	2.4-4.1	3	7.6 ± 3.0	6.5	5.5-9.0	3	0.7 ± 0.1	0.6	0.6-0.7	3
Mid	0.9 ± 0.2	0.8	0.7-1.1	3	3.5 ± 0.5	3.7	3.3-3.8	3	0.4 ± 0.1	0.4	0.4-0.5	3
Bot	1.0 ± 0.8	0.4	0.4-1.2	3	3.3 ± 1.3	2.4	2.4-3.8	3	0.34 ± 0.05	0.3	0.3-0.4	3
Brine	23.8 ± 3.5	25.3	22.5-25.7	11	56.7 ± 7.2	58.5	55.3-61.7	11	2.8 ± 0.4	2.9	2.6-2.9	11
SW	24.7 ± 3.4	25.2	22.5-27.5	5	59.0 ± 7.8	58.1	53.4-67.1	5	2.84 ± 0.5	2.8	2.4-3.4	5
Sample	Ammonium (μM)											
	avg ± SD	median	IQR	n								
Top	0.9 ± 0.2	0.9	0.8-1.0	3								
Mid	0.8 ± 0.1	0.9	0.8-0.9	3								
Bot	0.5 ± 0.2	0.5	0.4-0.6	3								
Brine	1.6 ± 0.2	1.6	1.5-1.7	11								
SW	1.7 ± 0.2	1.8	1.5-1.8	5								

Chl-a, POC and PON. Chl-a, POC and PON concentrations in sea ice typically exhibit significant seasonal variability, influenced by factors such as light availability, nutrient supply, and ice structure

(Arrigo and Thomas, 2004; Fripiat et al., 2017; Lund-Hansen et al., 2024). Chl-a, POC and PON values are generally low in winter due to reduced biological activity; they increase by several orders of magnitude during the spring bloom and decline following the bloom's demise in summer. Reported Chl-a concentrations in Antarctic sea ice range from 0.6 to 10 100 μg L^{-1}, spanning from levels characteristic of oligotrophic oceanic waters to some of the highest biomass values reported in any aquatic environment (Lim et al., 2025). During the PolarChange cruise, we observed Chl-a concentrations systematically below 1 μgL^{-1} in sea ice, which is extremely low compared to historical ice core data in Antarctic pack ice (Meiners et al., 2012) and in the lower range of values reported for land fast ice at this season (Meiners et al., 2018). Chl-a distribution peaked in the bottom sea ice and was several times higher compared to seawater concentration and brines (Figure 2A, C, Table 1). Similarly, POC exhibited higher concentrations in sea ice and brines than in seawater (Figure 2B, Table 1); however, this observation is limited to a single sea ice core. The highest POC concentrations were observed in the bottom section of a sea ice sample (47.0 μM), which corresponded to an enrichment factor of 1 256% relative to the surrounding seawater (Figure 2C, Table S1). PON concentration in ice and brine ranged from 0.8 to 2.1 and 0.5 to 1.2 μM, respectively, and was systematically higher compared to the underlying seawater (0.7 ± 0.3 μM, n = 4; Figure 2B, Table 1). The highest PON concentration was detected in a sea ice bottom section (2.1 μM), corresponding to an enrichment factor of 462% relative to the adjacent seawater (Figure 2C, Table S1). Although Chl-a, POC and PON concentrations are significantly larger in sea ice compared to the surrounding water, these concentrations are extremely low compared to previous spring and early summer sea ice observations (Meiners et al., 2012; Dalman et al., 2025) and are at the lower end of values typically recorded in late summer (March) in the Southern Ocean (Kattner et al., 2004; Meiners et al., 2012; Dalman et al., 2025). By this stage of the seasonal cycle, primary productivity has typically declined following the peak bloom in late spring to early summer. This reduction is further compounded by ongoing sea ice ablation, which results in the loss of bottom ice algal communities and diminished habitat suitability for ice-associated microalgae. Extensive sea ice melt at this time leads to the physical degradation of the ice matrix, often resulting in brine channel enlargement and flushing. This melt-driven flushing likely expelled much of the remaining ice-associated biomass, including the biofilm attached to the melting ice walls of the brine channels, further contributing to the low Chl-a, POC and PON levels recorded. At this point, the POC is

mostly detrital material or residual algal biomass. The POC:Chl-a ratio was systematically above 400 in sea ice, indicative of senescent or non-living organic matter (Dalman et al., 2025).

Biofilm TEP. TEP concentrations revealed a clear vertical structure, with highest values in the bottom (range: 174–311 µg Xeq L^{-1}) and mid ice horizons (149–280 µg Xeq L^{-1}), followed by lower levels in the top ice (23–268 µg Xeq L^{-1}), brines (56–152 µg Xeq L^{-1}), and surrounding seawater (46–52 µg Xeq L^{-1}) (Figure 2G, Table 1). This pattern is consistent with previous observations during sea ice algal blooms, where the bottom ice supports elevated microbial and algal biomass, leading to substantial exopolymer substance (EPS) production and accumulation. These values are generally lower than previously reported TEP concentrations in Antarctic bottom ice during bloom or post-bloom periods (e.g., Dumont et al., 2009: TEP > 1 000 µg Xeq L^{-1} in bottom sea ice), likely due to the late-season timing and advanced ice degradation. Despite the modest concentrations compared to peak bloom scenarios, these data confirm that decaying sea ice remains a reservoir of gel-like organic material, which may play a role in modulating aggregation processes and microbial interactions during meltwater export.

Nano- and microplankton composition. Among the microplankton sea ice taxa identified, dinoflagellates were the most abundant taxa followed by diatoms. In both ice and seawater environments, we identified motile forms of dinoflagellates such as *Gyrodinium* spp., *Gymnodinium* spp., *Katodinium* spp., *Prorocentrum* spp., and *Protoperidinium* spp. Diatoms were especially abundant in the bottom layer of bulk ice, with *Fragilariopsis* spp. being the most dominant, followed by *Navicula* spp., *Actinocyclus* spp., *Eucampia* spp., *Nitzschia* spp. and *Pseudo-Nitzschia* spp. In addition, ciliates were identified in bulk ice, brine and seawater but were a lot less abundant compared to dinoflagellates and diatoms. Among nanoplankton, *Cryptomonas* spp. were also identified in each medium (bulk ice, brine and seawater) but represented less than 0.002% of the overall abundance (Figure 2H). The observed assemblage, dominated by dinoflagellates, is consistent with the current literature, which reports that as the season progresses toward late summer, melting and brine drainage lead to nutrient depletion. This results in a decline in large diatoms and a shift toward smaller, more motile taxa, including flagellate protists (e.g., dinoflagellates) and heterotrophic and mixotrophic microbes, such as heterotrophic dinoflagellates, ciliates and bacteria (Becquevort et al., 2009; Torstensson et al., 2015; van Leeuwe et al., 2018). These later-stage communities reflect a transition from autotrophic to heterotrophic dominance,

often fuelled by the degradation of organic matter accumulated earlier in the season. High abundances of small dinoflagellates were observed in sea ice and brines, including both filled and empty cysts of the dinoflagellate *Polarella glacialis* and the archaemonad (chrysophyte) *Litheusphaerella spectabilis*. These two taxa are extant fossilizable planktonic groups, indicators of the marginal ice-edge zone (Montresor et al., 1999; Riaux-Gobin and Stumm, 2006; Malinverno et al., 2016). The high abundance of cysts reveals the dynamic processes of excystment within sea ice, allowing the microorganisms to survive in this extreme habitat. These metabolic processes involve intracellular changes in key compounds (e.g., synthesis and degradation of cell-wall proteins, reserve compounds, osmolytes) and the release of EPS, which in turn influence the chemical composition of the sea ice and brines.

Bacterial abundances. Bacterial abundance was systematically higher in bulk ice compared to brines or seawater (Figure 2E, F, Table 1). While Chl-a and viruses were always enriched in the bottom ice layers compared to the sea ice upper sections, bacteria were equally distributed in the bulk ice layers with no particular enrichment in the bottom ones. These values ranging from 1.1 x 10^5 to 1.4 x 10^6 cells mL^{-1} are in agreement with densities ranging from 0.6 x 10^5 to 4.2 x 10^5 cells mL^{-1} reported in winter sea ice from the same area by Luhtanen et al. (2018) but on the lower range of value (i.e., up to 3 x 10^7 cells mL^{-1}) reported in summer bottom ice following the ice-algal bloom, in both Arctic and Antarctic sea ice (Krembs and Engel, 2001; Thomas et al., 2001).

Microbiological components (protists, bacteria, viruses) develop and concentrate in brine inclusions (Legendre et al., 1991). It is therefore unexpected to observe biomass indicators (i.e., Chl-a, POC and PON) in higher concentrations in bulk ice compared to brines themselves (Figure 2A–G). However, microalgae produce EPS (i.e., TEP) that favors their attachment to the walls of brine inclusions (Gradinger and Ikävalko, 1998; Krembs et al., 2002). Low levels of Chl-a, POC and viruses in brine collected from sackholes support the idea that microbiological components are likely retained within biofilms (Collins and Deming, 2009; Deming and Young, 2017) formed along the brine channel walls and are thus not effectively recovered by the sackhole sampling method.

Viral abundances. Viruses play a crucial role in plankton mortality, and by impacting microbial communities, viruses may influence the cycling of organic compounds in sea ice. Total viral abundances were an order of magnitude higher in bulk sea ice (10^7 viruses mL^{-1}; Figure 2D, Table

1) than seawater (10^6 viruses mL^{-1}) and brines (10^6 viruses mL^{-1}). Similarly to Chl-a, total viral abundances peaked in the sea ice bottom (Figure 2D, F, Table S1). These values are in agreement with previously reported values ranging from 10^6 to 10^8 viruses mL^{-1} in the Ross Sea pack ice, in late summer (Gowing et al., 2004) and are slightly higher than those observed in sea ice samples collected during summer in the Weddell Sea, which ranged from 2 x 10^6 to 9 x 10^6 viruses mL^{-1} (Rocchi et al., 2022). However, they are lower than those reported in the same region of the Weddell Sea during winter (AWECS cruise, stations 515 and 517, in Luhtanen et al. (2018)). Viral abundances of similar magnitude were recorded in Arctic sea ice (9.0 x 10^6–1.5 x 10^8 viruses mL^{-1}) (Maranger et al., 1994).

Nutrients. Nutrient levels in sea ice vary over time, consistent with ecosystems governed by strong seasonal productivity. These changes are primarily influenced by biological processes such as uptake and incorporation into algal biomass, recycling through remineralization (Fripiat et al., 2017). Since nutrients, like sea salts, are excluded from the forming ice lattice, they accumulate in the brine network (Vancoppenolle et al., 2013). In winter, when biological activity is minimal, nutrient distribution closely mirrors the dissolved salts profile, primarily governed by physical transport processes such as brine convection and expulsion (Zhou et al., 2013). As spring arrives and sunlight increases, nutrient levels begin to decline, coinciding with the growth of microalgae within the ice (Fripiat et al., 2017).

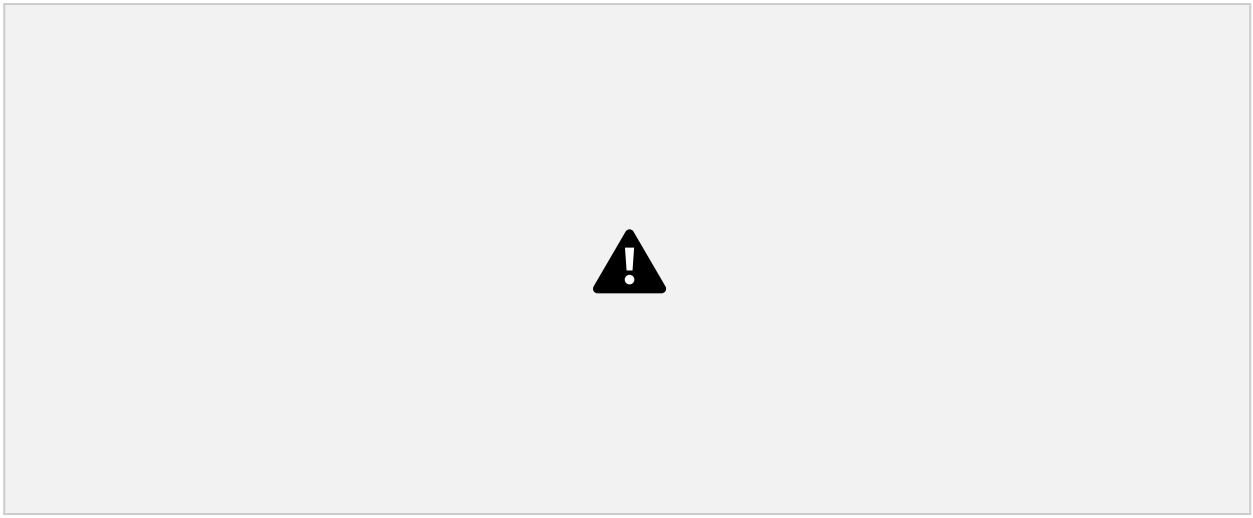

Figure 3. Nutrient concentrations in sea ice, brine and seawater. IQR Box plot of the concentration and enrichment factor of Nitrate plus nitrite **(A and E)**, silicate **(B and E)**, Phosphate **(C and E)** and ammonium **(D and E)** for the top, middle (Mid) and bottom (Bot) ice layers, brine and seawater. Box plots show the interquartile range (IQR; 25th–75th percentile), with the horizontal line indicating the median and whiskers extending to 1.5 × IQR. The number of data points is reported in Table 1.

Overall, the four ice stations were depleted in nutrients compared to seawater, with relatively low concentrations falling in the range of summer bulk ice concentrations reported in Fripiat et al. (2017) (Figure 3 A–E). While nutrients were depleted in sea ice similarly to sea salts, some significant differences in their enrichment factors suggest the presence of biological recycling processes. First, we observed that the brines were slightly enriched in all macronutrients compared to salinity ($EF_{brine\ nutrients} > EF_{brine\ salinity}$, Figures 1C, 3E, Table S1). It is well documented that organic matter concentrations build up in sea ice from spring to summer, and cold-adapted bacteria are known to thrive in this specific environment (Dieckmann and Thomas, 2002; Thomas and Dieckmann, 2002; Meiners et al., 2004; Dumont et al., 2009; Bowman, 2015; Lund-Hansen et al., 2024). Bacterial activity and degradation of algal cells through lysis and mortality favor the remineralization of organic matter (Günther et al., 1999; Thomas and Dieckmann, 2002; Fripiat et al., 2017), facilitating the enrichment of nutrients compared to salinity. Secondly, we observed that bulk sea ice was slightly enriched in ammonium and P compounds compared to salinity and other macronutrients. The ammonium-to-nitrate + nitrite ratio (NH_4^+: $NO^-_{(2+3)}$) in bulk ice spans 0.2 to 1.4, while in seawater and brine it ranges from 0.06 to 0.07 μM. This shows an accumulation of ammonium in bulk sea ice compared to nitrate. Organic nitrogen in sea ice is remineralized to NH_4^+ (Riedel et al., 2007; 2008). NH_4^+ in senescent condition is not assimilated by biomass but rather adsorbed and retained onto EPS (Fripiat et al., 2017) in brine inclusions. Sea ice algae are known to have low cell N:P ratios, since they accumulate P-rich biomass during a short but intense algal bloom (Arrigo et al., 1999; Fripiat et al., 2017). Subsequent lysis of P-rich diatom release could explain the enrichment in P relative to other macronutrients (nitrate, nitrite, and silicate). Similar to ammonium, P compounds can be retained on brine biofilms (Roukaerts et al., 2021).

3.3 Alkylamines

MMA concentrations were below the detection limit in all the analysed samples, while pTMA, dTMA, dDMA and dDEA were detected in almost all sea ice, brines, and seawater samples (Figure 4, Table 2).

Table 2. Concentration of alkylamines, S-compounds and VOCs in sea ice, brine and seawater. The average ± standard deviation, the median concentrations, 25th and 75th percentile (IQR), and "n" sample number of key compounds (alkylamines, S-compounds and VOCs) in top, middle (Mid) and bottom (Bot) layers of sea ice, brines and seawater (SW) (na: not available).

Sample	**pTMA (nM)**				**dTMA (nM)**				**dDMA (nM)**			
	avg ± SD	median	IQR	n	avg ± SD	median	IQR	n	avg ± SD	median	IQR	n
Top	73.1 ± 46.1	72.5	44.8-101.2	3	11.5 ± 6.0	10.1	7.5-14.7	3	18.8 ± 5.3	17.8	15.3-21.7	3
Mid	na	na	na	0	na	na	na	0	na	na	na	0
Bot	83.2 ± 69.7	36.4	33.9-109.1	3	819.2 ± 1023.3	155.3	96.4-1209.9	3	34.9 ± 26.4	20.7	16.3-46.3	3
Brine	34.4 ± 20.3	25.3	22.0-39.1	7	22.6 ± 20.2	11.1	5.7-41.9	8	14.4 ± 7.3	12.1	0-14.8	8
SW	25.1 ± 10.3	21.6	21.5-25.7	5	13.4 ± 8.8	14.4	8.1-18.4	5	15.4 ± 3.9	14.1	11.7-19.8	5
Sample	**dDEA (nM)**				**DMSP (nM)**				**DMS (nM)**			
	avg ± SD	median	IQR	n	avg ± SD	median	IQR	n	avg ± SD	median	IQR	n
Top	10.0 ± 1.1	10.7	9.5-10.7	3	6.6 ± 5.1	3.9	3.0-8.9	3	0.2 ± 0.1	0.2	0.1-0.3	5
Mid	na	na	na	0	29.3 ± 18.8	16.8	16.0-36.0	3	1.6 ± 1.5	1.1	0.1-3.6	6
Bot	20.6 ± 13.8	11.9	10.8-26.0	3	129.1 ± 126.2	126.2	105.0-151.0	3	8.2 ± 1.6	8.9	8.1-8.9	5
Brine	7.4 ± 0.5	7.5	6.9-7.6	8	21.7 ± 9.4	20.4	17.4-23.1	14	2.2 ± 1.8	1.2	0.8-2.6	14
SW	8.1 ± 1.0	8.5	7.8-8.8	5	17.4 ± 3.0	19.3	14.2-20.2	5	0.6 ± 0.1	0.6	0.8-1.0	5
Sample	**MeSH (nM)**				**Isoprene (nM)**				**Acetone (nM)**			
	avg ± SD	median	IQR	n	avg ± SD	median	IQR	n	avg ± SD	median	IQR	n
Top	0.06 ± 0.02	0.05	0.04-0.07	5	1.19 ± 0.28	1.21	0.96-1.50	5	58.0 ± 12.2	57.8	48.2-58.9	5
Mid	0.21 ± 0.14	0.19	0.08-0.28	6	0.84 ± 0.49	0.89	0.28-1.25	6	51.4 ± 23.8	43.6	30.9-74.2	6
Bot	0.64 ± 0.13	0.64	0.51-0.74	5	0.57 ± 0.29	0.54	0.29-0.88	5	39.1 ± 21.6	24.4	23.7-49.2	5
Brine	0.43 ± 0.18	0.39	0.31-0.54	14	0.16 ± 0.07	0.16	0.11-0.20	14	14.2 ± 5.4	14.6	9.3-16.9	14
SW	0.26 ± 0.10	0.27	0.26-0.27	5	0.07 ± 0.02	0.07	0.05-0.08	5	5.6 ± 1.1	5	4.7-5.7	5
Sample	**Benzene (nM)**				**Toluene (nM)**				**Xylene (nM)**			
	avg ± SD	median	IQR	n	avg ± SD	median	IQR	n	avg ± SD	median	IQR	n
Top	0.30 ± 0.09	0.27	0.25-0.29	5	1.26 ± 0.30	1.18	1.18-1.44	5	0.67 ± 0.23	0.59	0.51-0.78	5
Mid	0.25 ± 0.08	0.25	0.19-0.29	6	1.25 ± 0.95	0.83	0.73-1.31	6	0.59 ± 0.17	0.57	0.50-0.66	6
Bot	0.24 ± 0.10	0.24	0.17-0.26	5	1.50 ± 1.27	0.87	0.51-2.28	5	0.61 ± 0.24	0.55	0.47-0.69	5
Brine	0.17 ± 0.05	0.15	0.14-0.16	14	0.42 ± 0.13	0.42	0.33-0.46	14	0.42 ± 0.11	0.37	0.36-0.42	14
SW	0.09 ± 0.05	0.07	0.05-0.08	5	0.19 ± 0.14	0.13	0.12-0.13	5	0.22 ± 0.10	0.19	0.18-0.19	5

The total (dissolved + particulate) alkylamine average concentration in surface seawater was 62.0 ± 7.8 nM, which is higher than previous observations by Dall'Osto et al. (2017; 2019). pTMA, with a median concentration of 21.6 nM (IQR 21.5-25.7) (Table 2), represented 40.4 ± 16.7% of the total alkylamines and contributed to the surface seawater PON and POC up to 3.2 ± 1.0% and 1.2 ± 0.4%, respectively. Particulate concentrations in our surface seawater samples were higher than those reported by Rocchi et al. (2025) at 4 m depth in the same area and period. Vaqué et al. (2021) documented substantially elevated microbial activity within the uppermost metre of the water column relative to deeper layers (4 m depth) during the same season and region. This intensified viral–microbial activity may therefore account for the higher particulate concentrations observed in our near-surface samples. Dissolved amines (dDMA+dTMA+dDEA) contributed up to 60% of the total alkylamines, with dDMA and dTMA being the most abundant species with median concentrations of 14.1 nM (IQR 11.7-19.8) and 14.4 nM (IQR 8.1-18.4), respectively (Table 2). dDEA was the least abundant alkylamine (13.3 ± 2.4% of the total amine) with a median concentration of 8.5 nM (IQR 7.8-8.8) (Table 2).

Total alkylamine concentrations were substantially higher in sea ice than in seawater (Figure 4A). This was especially true for the bottom sea ice (Figure 4A, B). This pattern aligns with the vertical distributions of Chl-a, POC, and viruses, which also peaked in the bottom layers. The remarkably high amine levels observed in the bottom sea ice are likely due to release by microbiota potentially embedded in biofilms within the brine channels of sea ice.

Similarly to seawater, pTMA and dTMA were the most abundant forms of alkylamines in sea ice, followed by dDMA and dDEA (Figure 4C, Table 2). Indeed, TMA has been identified as the primary amine released during degradation of quaternary N-precursors (glycine betaine, choline, trimethylamine N-oxide (TMAO)), and bacteria may subsequently facilitate its conversion into DMA and MMA (Mausz and Chen, 2019; van Pinxteren et al., 2019; Fitzsimons et al., 2023; Rocchi et al., 2025). While in seawater samples pTMA was the only methylamine detected in particulate form (Rocchi et al., 2025), pDMA was detected in one of the bottom sea ice samples, with a concentration of 9.5 nM. In the top and bottom sections of the sea ice cores, pTMA represented 2.0 and 1.5% of PON and 0.2 and 0.2% of POC, respectively.

Regarding the concentrations of total dissolved alkylamines, they varied widely within brines and sea ice, from 6.7 nM in a brine sample up to 2 376.7 nM in a bottom sea ice sample. This large range was due to the exceptionally high dTMA level (2 264.7 nM) in one of the bottom sea ice samples. In this sample, we observed a high abundance of archaeomonad and *Polarella glacialis* cysts, previously described in Antarctic sea ice (Montresor et al., 1999; Riaux-Gobin and Stumm, 2006), with a predominance of empty archaeomonad cysts. Empty cysts indicate that the formerly resting cells had recently excysted into vegetative, swimming cells, which subsequently migrated from the bottom of the sea ice into the underlying seawater. The intense metabolic processes associated with this transformation involve active protein and enzyme activity that might lead to elevated TMA concentrations. In the other bottom sea ice samples, which showed lower amine concentrations, only full cysts were present, indicating that excystment had not yet begun. Further research is needed to determine whether microalgal excystments are especially prone to the production and accumulation of alkylamines.

This study provides the first evidence of particulate and dissolved alkylamines in sea ice and brine samples. To date, the only published reference reporting the presence of amines in sea ice is Dall'Osto et al. (2019), in which total dissolved methylamine concentrations (sum of MMA, DMA and TMA) were measured in two melted sea ice samples. The reported concentrations (6.5 to 10.8 nM) were substantially lower than those observed in the present study. It must be noted that their samples were artificially bubbled for aerosolization for 24 hours before analysis, likely resulting in significant degassing and underestimation of real concentrations.

In this study, we observed markedly elevated Σ(alkylamines):Chl-a ratios in sea ice (~1 000) compared to seawater (346). This high ratio suggests either enhanced production or greater preservation of alkylamines within the ice. Similar to other organic compounds, the alkylamine concentrations in brines were lower than those in sea ice (Figure 4, Table 1), indicating that while these compounds were produced in situ in brine channels, they were retained within the biofilm and did not drain out of the ice easily. Sea ice thus acted as a reservoir for alkylamines, despite late-season flushing conditions. In sea ice, a dynamic N cycle governs the uptake and transformation of inorganic N, with nitrate accumulating through winter (Fripiat et al., 2017). As the ice warms, growing microalgae assimilate nitrate (Fripiat et al., 2015), leading to the production of organic N compounds (i.e., amino acids, proteins, N-osmolytes) and nitrate depletion. Since brine

stratification restricts nitrate replenishment from the underlying seawater, the dominant N pool shifts seasonally from inorganic to organic forms (Fripiat et al., 2014; 2015). Alkylamines may represent a previously unrecognized component of this organic N pool, potentially contributing to N cycling in sea ice. This might explain why MMA concentrations were below the detection limit, as MMA is, compared to TMA, DMA, and DEA, preferentially assimilated by sea ice microorganisms in N-depleted conditions (Stein, 2017, and references therein; Taubert et al., 2017). This preference is supported by the simplicity and wider occurrence of metabolic pathways for MMA utilization in comparison to the scarcer and more complex pathways required for the assimilation of other methylamines (Lidbury et al., 2017; Taubert et al., 2017; Wang et al., 2021).

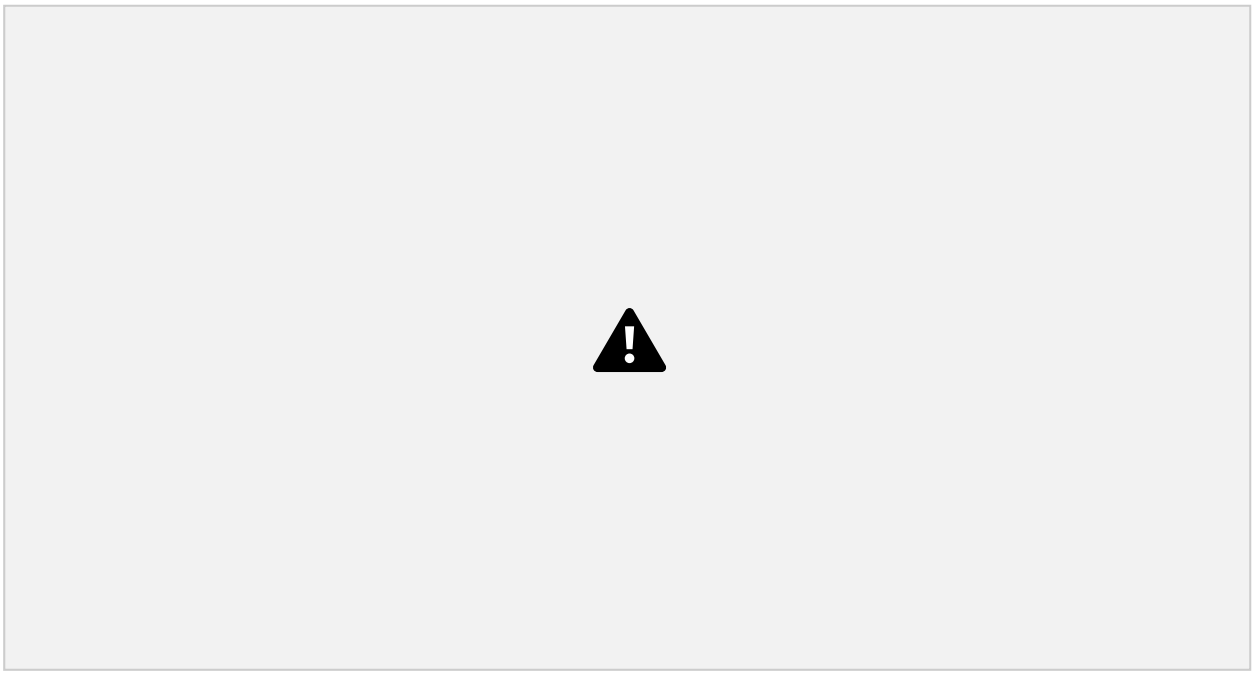

Figure 4. Alkylamines distribution in sea ice brine and seawater. IQR Box plots of total (particulate + dissolved) alkylamine concentrations (pTMA, dTMA, dDMA, dDEA) **(A)** and their enrichment factors **(B)**, along with the average relative abundance of each alkylamine with respect to the total **(C)** in the top (n =3) and bottom (Bot, n = 3) ice layers, brine (n = 8) and seawater (note that for alkylamine there were no middle-ice samples). Box plots show the interquartile range (IQR; 25th–75th percentile), with the horizontal line indicating the median and whiskers extending to 1.5 × IQR.

3.4 **Methanethiol, DMS and DMSP**

DMSP degradation leads to the production of DMS and MeSH via cleavage and demethylation, respectively (Stefels et al., 2007; Moran et al., 2012; Teng et al., 2021; Hopkins et al., 2023). To our knowledge, MeSH has never been studied in sea ice; conversely, DMSP and DMS concentration distributions have been the focus of numerous works in Antarctic sea ice (Trevena and Jones, 2006; Zemmelink et al., 2006; 2008; Tison et al., 2010; Nomura et al., 2012; Stefels et al., 2012; Damm et al., 2016; Carnat et al., 2018). These studies have shown that seasonal variations in DMSP and DMS in sea ice are closely linked to changes in the biomass and composition of microalgal assemblages (Tison et al., 2010). During winter, low algal abundance and activity result in minimal DMSP production (Carnat et al., 2014) and, consequently, low DMS concentrations. As spring arrives, ice-associated microalgae proliferate, leading to increased Chl-a levels and elevated DMSP concentrations. As algal blooms wane and cells senesce or lyse, DMSP is released into the brine and degraded to DMS. The further evolution of these compounds throughout the summer season is less well documented, as summer sea ice is undersampled (Burke et al., 2024).

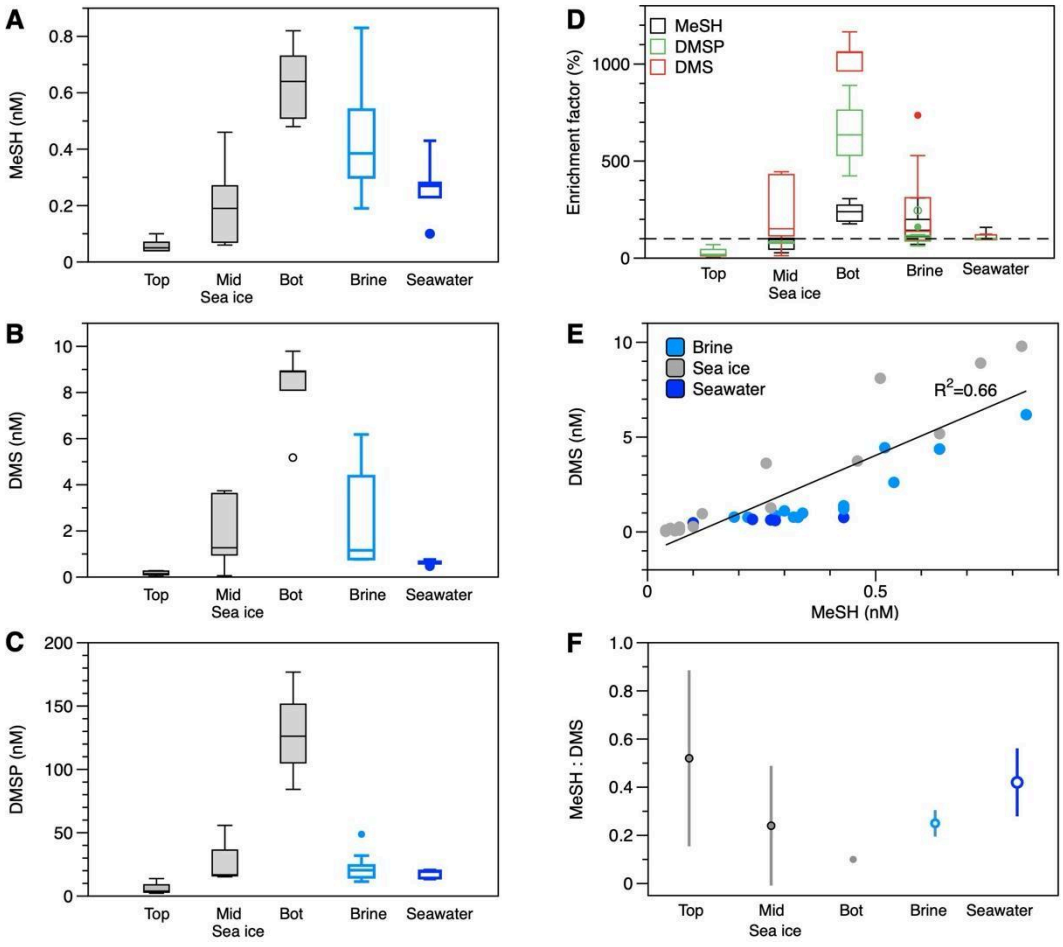

Figure 5. Sulfur compounds in sea ice, brine and seawater. IQR Box plots of MeSH (**A**), DMS (**B**), and DMSP (**C**) concentrations (nM) and their enrichment factors (%, **D**) in top (n = 6), middle (Mid, n = 5), and bottom (Bot, n = 5) ice layers, brine (n = 14) and seawater (n = 5). Along with the relationships between MeSH and DMS (**E**) and the ratio between MeSH:DMS (**F**). Box plots show the interquartile range (IQR; 25th–75th percentile), with the horizontal line indicating the median and whiskers extending to 1.5 × IQR.

Surface seawater DMSP and DMS concentrations ranged from 13.4 nM to 20.5 nM and from 0.48 nM to 0.76 nM, respectively. These concentrations are in agreement with concentrations reported in summer from surface water of sea ice-leads in the Weddell Sea by Zemmelink et al. (2005) and near the lower end of the range observed in summer by Rellinger et al. (2009), Stefels et al. (2018), Li et al. (2024) in the northern Weddell Sea.

In sea ice, DMSP and DMS concentrations showed a steep vertical gradient, peaking at the bottom, with enrichment factors above 500% and 1 000%, respectively (Figure 5, Tables 2 and S1). While the DMSP and DMS concentrations in bulk sea ice (2.20–176.80 and 0.03–9.79 nM, respectively) were higher than in the surrounding surface waters, they were remarkably low compared to those previously encountered during sea ice algal bloom and senescence (Trevena and Jones, 2006; Tison et al., 2010; Carnat et al., 2014). Zemmelink et al. (2008) reported DMSPt concentrations as high as 11 352 nM in the productive surface layer of second-year ice during Austral Spring (November-December 2004) in the Weddell Sea. Other authors have reported DMSP concentrations ranging from less than 5 to around 1 660 nM (Trevena et al., 2003), with average concentrations in the order of 100 to 300 nM. Our measurements fall at the lower range of their observations. Similarly, past studies reported high mean DMS concentrations of between 7 and 60 nM and up to 1 430 nM during the sea ice bloom (Trevena and Jones, 2006; Tison et al., 2010; Carnat et al., 2016), while the range observed here is about an order of magnitude less than that. Overall, this indicates that the sea ice sampled here was depleted in many of these biological sulfur compounds due to the late season. However, the distribution patterns with significant enrichment in the bottom ice layer were similar to those observed during the peak productivity season.

The MeSH concentration in seawater ranged from 0.10 nM to 0.43 nM, which were at the low end of measurements conducted around the Antarctic Peninsula during the same cruise (Wohl et al.,

2024) but similar to previous surface seawater measurements near sea ice in the Arctic (0.02–0.53 nM) (Gros et al., 2023). These measurements also compare well to the mean reported in temperate and warmer environments (Kettle et al., 2001; Kiene et al., 2021; Wohl et al., 2023a; 2024; Deschaseaux et al., 2025). MeSH concentrations were twice as high in bottom bulk sea ice compared to the surrounding seawater, yielding a median enrichment factor of 218% (IQR 190-273) (Figure 5A, D, Tables 2 and S1). The brines were also enriched (EF = 143%) while the middle and top sea ice layers were slightly depleted compared to the surrounding seawater.

The vertical variability of MeSH in sea ice provides insight into its sources, distribution, and production pathways. Elevated MeSH concentrations in bottom ice layers closely followed the distribution of microorganism-related components (Chl-a, POC, PON, viruses) and DMSP, indicating a strong biological origin. High dinoflagellate abundance, together with the presence of ciliates and viruses, further supports microbial production by promoting DMSP-rich cell lysis. MeSH also showed a strong positive correlation with DMS across all samples ($R^2 = 0.66$, $n = 35$), consistent with the interpretation that both compounds largely derive from DMSP degradation (Figure 5E). In addition, MeSH-producing bacteria such as members of the *Roseobacter* and *SAR11 clades*, known to generate MeSH via the demethylation pathway (Howard et al., 2006; Reisch et al., 2011; Teng et al., 2021), have previously been reported in sea ice (Brinkmeyer et al., 2003).

The exceptionally low concentrations of the three sulfur compounds at the top layers of the ice cores were associated with low biological activity. Chl-a concentration in the upper layers was approximately seven times lower than in the bottom layers. In addition, the upper sea ice layers were exposed to high light, enhancing photochemical sinks that could keep sulfur compound concentrations low. Since the upper layers were somewhat isolated from the bottom layers due to low brine connectivity (i.e., brine volume < 5% in the middle of the ice core, Figure 1A), and given that the lifetime of MeSH in seawater is short (on the order of hours, Kiene (1996)), MeSH was most likely produced in situ at the different depths rather than diffusing from the bottom.

The lower concentrations at the top layers of the ice compared to the surrounding seawater also suggest that the ice-to-air fluxes of DMS and MeSH at this time of year were very small. The MeSH:DMS concentration ratios encountered in surface seawater and top ice (0.2–0.9; Figure 5F) imply that the contribution of MeSH to the emission of volatile methylated sulfur

(MeSH:(MeSH+DMS)) from the Weddell Sea in late summer fell at the upper end of the global latitudinal pattern (Wohl et al., 2024). However, the take-off of DMS concentration in the bottom ice was not accompanied by a proportional increase in MeSH, resulting in a lower MeSH:DMS ratio (0.1; Figure 5F). We can only speculate that the algal and bacterial growing conditions and assemblage composition at the bottom of the sea ice favored DMS production over MeSH. As a matter of fact, this agrees with the few high DMS events observed in surface seawater around the Antarctic Peninsula during the same cruise, where DMS concentrations above 8 nM typically resulted in lower MeSH:DMS ratios (Wohl et al., in preparation). It has long been suggested that a high availability of DMSP to bacteria in nutrient-limited conditions would favor bacterial DMSP catabolism via DMSP lyases (leading to DMS production) over the demethylation pathway (leading to MeSH) (Kiene et al., 2000; Simó, 2001). Also, a larger presence of DMSP-lyase-containing microalgae in the bottom ice would favor DMS production. Although compared to the upper section, the bottom ice hosted a reduced proportion of dinoflagellates (usually DMSP-lyase-harbouring organisms) in favor of diatoms (organisms that do not harbor DMSP-lyase) (Figure 2H), the much higher biomass at the bottom still implies a greater absolute biomass of dinoflagellates.

3.5 VOCs

This study presents the first quantitative measurements of a range of VOCs in polar sea ice, including an oxygenated VOC (acetone), a biogenic VOC (isoprene), and volatile aromatic hydrocarbons (BTX).

The acetone concentration in the surrounding seawater ranged from 4.5 to 7.7 nM, which is consistent with previously reported values for the Southern Ocean away from the ice edge (Wohl et al., 2020). In sea ice, acetone concentrations increased from the bottom (median 24.4 (IQR 23.7-49.2) nM) towards the top layers (median 58.0 (IQR 48.2-59.0) nM) with brine samples showing a lower concentration (median 14.5 (IQR 9.3-16.9) nM) (Figure 6A, Table 2). The enrichment factor for acetone exceeded 700% in all sea ice fractions and peaked above 1 000% in top layers (Figure 6C, Table S1). Overall, acetone concentrations were consistently higher in the ice matrix than in the surrounding seawater (Figure 6C, Table 2). This suggests active acetone production in sea ice or other factors favoring its accumulation. Its vertical distribution in sea ice

(Figure 6A, Table 2) peaking in the surface layers follows the vertical light gradient of the sea ice cover, suggesting that the dominant source of acetone in sea ice was photochemical production, consistent with observations from other marine environments (Dixon et al., 2013; Zhu and Kieber, 2018).

Concerning isoprene, the median concentration within sea ice were very high compared to seawater and increased from the bottom layers (median 0.54 (IQR 0.29-0.88) nM) towards the top layers (median 1.21 (IQR 0.96-1.50) nM) with brine concentrations systematically below 0.20 nM (Figure 6B, Table 2). Isoprene exhibited a very high enrichment factor in sea ice (EF > 1 000%, Figure 6C, Table S1) compared to the surrounding seawater, which had a concentration below 0.09 (Figure 6B). The dissolved concentrations in seawater were within the upper range of previously reported concentrations for the Atlantic sector of the Southern Ocean and the Weddell Sea (Rodríguez-Ros et al., 2020) or for the Arctic sea ice zone (Wohl et al., 2022). Isoprene is known to be mainly produced by phytoplankton (Shaw et al., 2010) and in the open ocean generally correlates quite well with Chl-a (Wohl et al., 2020). However, the vertical isoprene profile observed here, peaking in the upper sea ice layers, contrasts with the Chl-a maximum located in the bottom ice. These elevated concentrations and the atypical vertical distribution suggest that isoprene production in sea ice is driven by unknown physiological and environmental factors. While high light exposure combined with low salinity and nutrient stress has been shown to enhance isoprene production in seawater (Booge et al., 2018), further investigation is needed to confirm that such environmental conditions in sea ice could drive high isoprene production in surface layers.

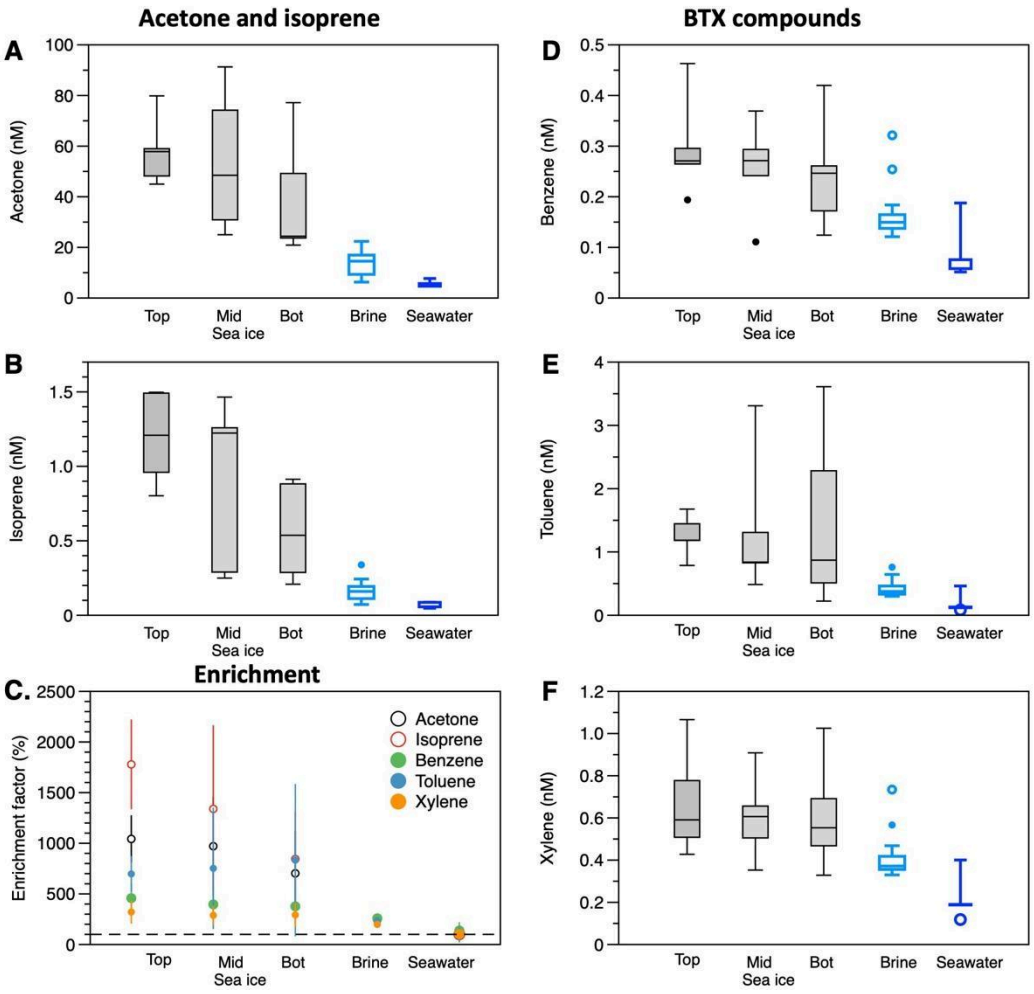

Figure 6.VOC distribution in sea ice, brine and seawater. IQR Box plots of the concentrations (nM) of VOCs (Acetone, **A**; Isoprene, **B**; Benzene, **D**; Toluene, **E**; and Xylene, **F**) and their enrichment factors, % (**C**) in top (n = 6), middle (Mid, n = 5), and bottom (Bot, n = 5) ice layers, brine (n = 14) and seawater (n = 5). Box plots show the interquartile range (IQR; 25th–75th percentile), with the horizontal line indicating the median and whiskers extending to 1.5 × IQR.

Seawater median concentrations of benzene, toluene and xylene (Table 2) reported here were generally on the upper end of the range reported by Wohl et al. (2023b) for the Southern Ocean, away from the sea ice edge (Figure 6D–F, Table 2). All BTX concentrations were higher in sea ice than seawater, with toluene displaying the highest enrichment factor (Figure 6C). Enrichment factors for toluene exceeded 1 600% in the bottom sea ice fraction, 1 000% in the top, 600% in the middle, and 300% in the brines (Table S1). Across the ice layers, the median benzene concentration

ranged from 0.24 to 0.27 nM (Table 2) and decreased slightly from the top to bottom layers. While median concentrations of toluene also decreased from the top towards the bottom layers (median 1.18 (IQR 1.18-1.44) nM), the bottom layers exhibit a greater variability and host the highest concentrations (Figure 6E, Table 2). All ice layers exhibited relatively uniform xylene concentrations, with a median concentration below 0.60 nM, while brine samples had a lower median of 0.37 nM (Table 2).

The much higher BTX concentrations in sea ice compared to seawater indicate that sea ice conditions favour BTX accumulation and that sea ice may act as a source of BTX to the atmosphere. While the origin of these compounds in pristine seawater is still under investigation, experimental studies (Romoli et al., 2011; Misztal et al., 2015; Lemfack et al., 2018; Rocco et al., 2021) and recent observations in polar seawater (Wohl et al., 2023b) have shown that phytoplankton and bacteria can produce BTX, with degradation of aromatic amino acids representing a likely pathway (Padaki et al., 2025). Although the enrichment of BTX in sea ice supports a biological origin, the absence of clear vertical gradients and the lack of correspondence with Chl-a suggest that BTX levels cannot be explained solely by phytoplankton biomass and warrant further investigation.

Accumulation of these VOCs toward the ice surface layers suggests that they could be released into the atmosphere. Air-ice CO_2 flux studies demonstrated that sea ice can episodically exchange gases with the atmosphere, depending on factors such as ice permeability, brine transport, and snow cover (Delille et al., 2014; Van der Linden et al., 2020). At this time of year, sea ice top layers were permeable (brine volume > 5%, Figure 1A), potentially allowing VOCs to volatilize into the atmosphere, where it can influence atmospheric chemistry. Recent ambient air measurements indicate that the Southern Ocean sea ice zone may be a significant source of isoprene to the atmosphere (Ferracci et al., 2024). In that study, atmospheric isoprene concentrations could not be correctly simulated by models constrained solely by surface-ocean concentrations, pointing to (an) overlooked isoprene source(s). Our results suggest that emissions from the top of the sea ice could be one such additional source.

3.6. Brine sackhole sampling bias

Since biogeochemical compounds are concentrated in brine inclusions and not incorporated into the ice crystal lattice, brine should contain higher concentrations than in bulk ice; theoretically, brine concentrations can be estimated by dividing bulk ice concentrations by the brine volume fraction.

It is well documented that the liquid fraction of brine collected by sackhole tends to underrepresent particulate components, such as Chl-a and POC (Becquevort et al., 2009; Miller et al., 2015; Lannuzel et al., 2016; Duprat et al., 2019). This underrepresentation occurs because Chl-a and POC are primarily associated with biomass (including living and detrital particles) that are preferentially adsorbed onto the ice walls and embedded in gelatinous biofilm matrix. In addition, these components are often too large to be mobilised efficiently through the narrow brine channels that drain into the sackhole.

In contrast, sackhole sampling is normally well suited for analysing dissolved compounds and yields higher concentrations of dissolved salts and macronutrients in brine than in bulk ice (Figures 1, 3). However, we still observed a large discrepancy between brine and bulk ice concentrations of dissolved organic compounds, including DMS(P), MeSH, alkylamines, and VOCs. These were significantly depleted in brines compared to bulk ice, suggesting that they were not fully recovered in the brine sampled by sackhole. This underrepresentation of compounds in sackhole-derived brine suggests two possible scenarios leading to a retention: (i) either biogeochemical processes occur primarily within the biofilm matrix, with only limited release of dissolved compounds into the surrounding brine, or (ii) biogeochemical processes take place externally (i.e., in the free moving brines), but polar chemical interactions and physico-chemical affinities promote the retention of these compounds within the biofilm structure. It should be noted that concentration differences between sackhole brines and melted bulk sea ice have also been reported for dissolved iron and ammonium in Antarctic sea ice, suggesting potential adsorption onto biofilms (Lannuzel et al., 2016; Fripiat et al., 2017).

4. Sources of volatile compounds in sea ice

While the sampled sea ice was clearly in a decaying state and had been washed out of most of its solutes and its biomass, sea ice bottom layers showed systematic enrichment in MeSH and alkylamines with concentrations significantly higher than in the surrounding seawater. Their distribution showed a strong vertical gradient, mirroring that of the microbiological components,

especially Chl-a and POC concentrations and viral abundance. The enrichment in bottom sea ice suggests that these compounds are not controlled by physical transport processes that regulate dissolved solutes but rather are produced in situ by microbial activity.

At the time of sampling (late summer), the sea ice exhibited extremely low biomass compared to typical spring conditions, yet still retained decaying organic matter, as well as diatoms, dinoflagellates, viruses, and bacteria. The accumulation of DMSP, DMS, and MeSH in bottom sea ice suggests that these compounds continue to be produced and cycled even in decaying ice, long after the peak algal bloom has ended. The occurrence of MeSH indicates that sea ice represents a hitherto unaccounted source of this compound to the atmosphere. Given the similarities in the vertical gradients of DMSP, DMS, and MeSH, and the well-recognised link between DMSP and the growth of sea ice algae, we hypothesise that MeSH must peak during the spring sea ice algal bloom, with concentrations well above those reported in this study.

Regarding N-compounds, our results suggest that dissolved and particulate alkylamines in sea ice may originate from protists and their cysts, which may actively or passively (i.e., through viral lysis) release alkylamine or N-osmolyte precursors for bacterial transformations. This underscores the entangled biological processes underlying polar alkylamine dynamics, which warrant further investigation. All in all, this study confirms that Antarctic marine microbiota is a primary source of alkylamines (Dall'Osto et al., 2019; Rocchi et al., 2025) and that sea ice acts as a reservoir and source of low-molecular-weight N-containing compounds (Dall'Osto et al., 2017; 2019; Rinaldi et al., 2020).

The concentrations of all VOCs were higher in sea ice than in seawater or brine and showed enrichment factors largely superior to salinity. This suggests that these compounds are regulated by processes other than physical transport alone and points towards biotic and abiotic factors controlling their concentrations in sea ice. Remarkably, the vertical profiles of the target VOCs did not parallel (or were even opposite to) those of the sulfur compounds. In contrast to these and alkylamines, VOCs could not be linked straightforwardly to the bulk sea ice microbiological distribution, since no VOCs consistently accumulated in the bottom layers. For acetone, the increasing gradient towards the top suggests that the dominant source is photochemical degradation of dissolved organic matter. While the process responsible for the vertical distribution of isoprene

and BTX compounds requires further research, the systemic accumulation of VOCs toward the ice surface layers suggests that these compounds can be exchanged with the overlying atmosphere.

5. Recommendations

Sea ice, one of the largest biomes on Earth, exchanges microbes, organic matter and nutrients with the surrounding ocean, thereby profoundly influencing marine ecosystem dynamics. This study highlights that sea ice is also a reservoir and potential atmospheric source of biogenic trace gases and aerosol precursors, with implications for atmospheric chemistry and climate. The mechanisms driving the production of reactive volatiles and aerosol precursors in sea ice likely involve microbial and photochemical processes within sea ice brines. Our findings on decaying sea ice at the end of the productive season suggest that the production of trace gases and aerosol precursors peaks earlier during the bloom and demise of ice-associated algae, as observed for better-known compounds like DMS. To better constrain the timing and pathways of such production, we recommend targeted sampling of sea ice during bloom initiation and senescence periods. Such efforts are essential for estimating ice-to-atmosphere trace gas emissions and for modelling their chemistry and climate impacts.

Author Contributions

O.C., A.R., C.W., M.D.O., E.B. and R.S. conceived and designed the research. A.R. and A.S. collected seawater samples. O.C., S.M., R.S., M.D.O. and C.W. collected sea ice cores and brines. A.R. processed and analysed the amine samples and generated amine data with the supervision of M.F.F. and P.A. C.W. measured volatile S-compounds and VOCs. Y.M.C. analyzed DMSP. M.V., D.V., E.L.S., E.B. and Y.M.C. collected samples and conducted biogeochemical, microscopy and flow cytometry analyses. T.B. collected TEP samples and analysed them. M.F.F provided essential resources for the amine analysis, B.D. contributed resources for sea ice and brine sampling and A.E. for TEP sampling and analysis. A.R. and O.C. performed the statistical analyses, generated the graphs, and drafted the first version of the manuscript. O.C., A.R., C.W., A.S., B.D., E.B. and R.S. contributed to data interpretation and manuscript writing. All authors participated in reviewing and editing the final version of the manuscript. All authors have approved the submission.

Acknowledgements

We would like to thank the crew of the RV *Hesperides* for the logistical support, making possible the data collection of this study. Special thanks to Mara Abad and Núria González Fernández for nutrient analyses at the Chemistry Service of the ICM-CSIC.

Financial Support

This research was funded by the Spanish Ministerio de Ciencia e Innovación (MICIN) through the POLAR CHANGE project (PID2019-110288RB-I00) granted to M.D.O., R.S., E.B. and M.V. and an the associated FPI grant (PRE2020-092994) to A.R.. Support was also provided by the European Research Council (ERC) under the European Union's Horizon 2020 research and innovation programme, through grant #834162 (SUMMIT) to R.S. Additionally, A.R. received funding from the European Social Fund (ESF) under the "Investing in your Future" initiative. We also acknowledge support from the Scientific Network PolarCSIC funded by the Consejo Superior de Investigaciones Científicas (CSIC), Spain, from the institutional support of the "Severo Ochoa Centre of Excellence" accreditation (CEX2024-001494-S) to the ICM-CSIC, and from the F.R.S-FNRS through research credit Sonatina (J.0060.22) and project Sea Ice Spray (T.0061.23). S.M., O.C. and B.D. were FRIA PhD student, postdoc and research associate, respectively, at the F.R.S.-FNRS. T.B. and A.E. were supported by the Helmholtz Association of German Research Centres.

Supporting Information

Yes
https://docs.google.com/document/d/1WSALTdxCv2lgxDJFPID8jXfGrwuZrY4a6fvO7Evcgmo/edit?tab=t.0

Data availability

The datasets supporting this study will be made publicly available via the Zenodo data repository. A DOI will be provided and included in the final version of the manuscript upon acceptance for publication.

References

Akenga PC, Fitzsimons MF. 2024. Automated method for the sensitive analysis of volatile amines in seawater. *ACS Earth Space Chem* 4(6): 2504–2510. doi:10.1021/acsestwater.4c00007

Arrigo KR, Robinson DH, Worthen DL, Dunbar RB, DiTullio GR, VanWoert M, Lizotte MP. 1999. Phytoplankton community structure and the drawdown of nutrients and CO_2 in the Southern Ocean. *Science* 283(5400): 365–367. doi:10.1126/science.283.5400.365

Arrigo KR, Thomas DN. 2004. Large scale importance of sea ice biology in the Southern Ocean. *Antarct Sci* 16(4): 471–486. doi:10.1017/S0954102004002263

Becquevort S, Dumont I, Tison J-L, Lannuzel D, Sauvée M-L, Chou L, Schoemann V. 2009. Biogeochemistry and microbial community composition in sea ice and underlying seawater off East Antarctica during early spring. *Polar Biol* 32(6): 879–895. doi:10.1007/s00300-009-0589-2

Booge D, Schlundt C, Bracher A, Endres S, Zäncker B, Marandino CA. 2018. Marine isoprene production and consumption in the mixed layer of the surface ocean – a field study over two oceanic regions. *Biogeosciences* 15(2): 649–667. doi:10.5194/bg-15-649-2018

Bowman JS. 2015. The relationship between sea ice bacterial community structure and biogeochemistry: a synthesis of current knowledge and known unknowns. *Elementa: Science of the Anthropocene* 3: 72. doi:10.12952/journal.elementa.000072

Brean J, Dall'Osto M, Simó R, Shi Z, Beddows DCS, Harrison RM. 2021. Open ocean and coastal new particle formation from sulfuric acid and amines around the Antarctic Peninsula. *Nature Geoscience* 14(6): 383–388. doi:10.1038/s41561-021-00751-y

Brinkmeyer R, Knittel K, Jürgens J, Weyland H, Amann R, Helmke E. 2003. Diversity and structure of bacterial communities in Arctic versus Antarctic pack ice. *Applied and Environmental Microbiology* 69(11): 6610–6619. doi:10.1128/AEM.69.11.6610-6619.2003

Brussaard CPD. 2004. Optimization of procedures for counting viruses by flow cytometry. *Applied and Environmental Microbiology* 70(3): 1506–1513. doi:10.1128/AEM.70.3.1506-1513.2004

Burke G, Wongpan P, Lannuzel D, Hayashida H. 2024. Data collation for climate-cooling gas dimethylsulfide in Antarctic snow, sea ice and underlying seawater. *Scientific Data* 11(1): 1185. doi:10.1038/s41597-024-04038-w

Carnat G, Brabant F, Dumont I, Vancoppenolle M, Ackley SF, Fritsen C, Delille B, Tison J-L. 2016. Influence of short-term synoptic events and snow depth on DMS, DMSP, and DMSO dynamics in Antarctic spring sea ice. *Elementa: Science of the Anthropocene* 4: 000135. doi:10.12952/journal.elementa.000135

Carnat G, Said-Ahmad W, Fripiat F, Wittek B, Tison J-L, Uhlig C, Amrani A. 2018. Variability in sulfur isotope composition suggests unique dimethylsulfoniopropionate cycling and microalgae metabolism in Antarctic sea ice. *Communications Biology* 1: 212. doi:10.1038/s42003-018-0228-y

Carnat G, Zhou J, Papakyriakou T, Delille B, Goossens T, Haskell T, Schoemann V, Fripiat F, Rintala J-M, Tison J-L. 2014. Physical and biological controls on DMS,P dynamics in ice shelf-influenced fast ice during a winter–spring and a spring–summer transitions. *Journal of Geophysical Research: Oceans* 119: 2882–2905. doi:10.1002/2013jc009381

Coggon MM, Stockwell CE, Claflin MS, Pfannerstill EY, Xu L, Gilman JB, Marcantonio J, Cao C, Bates K, Gkatzelis GI, Lamplugh A, Katz EF, Arata C, Apel EC, Hornbrook RS, Piel F, Majluf F, Blake DR, Wisthaler A, Canagaratna M, Lerner BM, Goldstein AH, Mak JE, Warneke C. 2024. Identifying and correcting interferences to PTR-ToF-MS measurements of isoprene and other urban volatile organic compounds. *Atmospheric Measurement Techniques* 17(2): 801–825. doi:10.5194/amt-17-801-2024

Collins RE, Deming JW. 2009. The potential for horizontal gene transfer in sea ice. *ISME Journal* 3: 193–202. doi:10.1038/ismej.2008.96

Corral AF, Choi Y, Collister BL, Crosbie E, Dadashazar H, DiGangi JP, Diskin GS, Fenn MA, Kirschler S, Moore RH, Nowak JB, Shook MA, Stahl CT, Shingler T, Thornhill KL, Voigt C, Ziemba LD, Sorooshian A. 2022. Alkyl amines in cloud water: a case study over the northwest Atlantic Ocean. *Environmental Science: Atmospheres* 2: 1534–1550. doi:10.1039/d2ea00117a

Dall'Osto M, Airs RL, Beale R, Cree C, Fitzsimons MF, Beddows D, Harrison RM, Ceburnis D, O'Dowd C, Rinaldi M, Paglione M, Nenes A, Decesari S, Simó R. 2019. Simultaneous detection of alkylamines in the surface ocean and atmosphere of the Antarctic sympagic environment. *ACS Earth and Space Chemistry* 3(5): 854–862. doi:10.1021/acsearthspacechem.9b00028

Dall'Osto M, Ovadnevaite J, Paglione M, Beddows DCS, Ceburnis D, Cree C, Cortés P, Zamanillo M, Nunes SO, Pérez GL, Ortega-Retuerta E, Emelianov M, Vaqué D, Marrasé C, Estrada M, Sala MM, Vidal M, Fitzsimons MF, Beale R, Airs RL, Rinaldi M, Decesari S, Facchini MC, Harrison RM, O'Dowd C, Simó R. 2017. Antarctic sea ice region as a source of biogenic organic nitrogen in aerosols. *Scientific Reports* 7(1): 6047. doi:10.1038/s41598-017-06188-x

Dall'Osto M, Vaque D, Sotomayor-Garcia A, Cabrera-Brufau M, Estrada M, Buchaca T, Soler M, Nunes S, Zeppenfeld S, van Pinxteren M, Herrmann H, Wex H, Rinaldi M, Paglione M, Beddows DCS, Harrison RM, Berdalet E. 2022. Sea ice microbiota in the Antarctic Peninsula modulates cloud-relevant sea spray aerosol production. *Frontiers in Marine Science* 9: 827061. doi:10.3389/fmars.2022.827061

Dalman LA, Meiners KM, Thomas DN, Deman F, Bestley S, Moreau S, Arrigo KR, Campbell K, Corkill M, Cozzi S, Delille B, Fransson A, Fraser AD, Henley SF, Janssens J, Lannuzel D, Munro DR, Nomura D, Norman L, Papadimitriou S, Schallenberg C, Tison J-L, Vancoppenolle M, van der Merwe P, Fripiat F. 2025. Observation-based estimate of net community production in Antarctic sea ice. *Geophysical Research Letters* 52(7): e2024GL113717. doi:10.1029/2024GL113717

Damm E, Nomura D, Martin A, Dieckmann GS, Meiners KM. 2016. DMSP and DMS cycling within Antarctic sea ice during the winter–spring transition. *Deep-Sea Research Part II: Topical Studies in Oceanography* 131: 150–159. doi:10.1016/j.dsr2.2015.12.015

Davie-Martin CL, Giovannoni SJ, Behrenfeld MJ, Penta WB, Halsey KH. 2020. Seasonal and spatial variability in the biogenic production and consumption of volatile organic compounds

(VOCs) by marine plankton in the North Atlantic Ocean. *Frontiers in Marine Science* 7: 611870. doi:10.3389/fmars.2020.611870

Delille B, Vancoppenolle M, Geilfus N-X, Tilbrook B, Lannuzel D, Schoemann V, Becquevort S, Carnat G, Delille D, Lancelot C, Chou L, Dieckmann GS & Tison J-L. 2014. Southern Ocean CO_2 sink: the contribution of the sea ice. *Journal of Geophysical Research: Oceans* 119: 6340–6355. doi:10.1002/2014JC009941

Deming JW, Young JN. 2017. The role of exopolysaccharides in microbial adaptation to cold habitats. *In:* Margesin R, ed. *Psychrophiles: From Biodiversity to Biotechnology.* Cham: Springer International Publishing. p. 259–284. doi:10.1007/978-3-319-57057-0_12

Deschaseaux ESM, Dunne E, Schulz KG, Eyre BD, Harrison DP. 2025. The central Great Barrier Reef as a net source of climatically relevant biogenic volatile organic compounds. *Journal of Geophysical Research: Oceans* 130(1). doi:10.1029/2024JC021192

Dieckmann G, Thomas D. 2002. Biogeochemistry of Antarctic sea ice. In: *Oceanography and Marine Biology: An Annual Review*. CRC Press. p. 143–169. doi:10.1201/9780203180594.ch3

Ditto JC, Huynh HN, Yu J, Link MF, Poppendieck D, Claflin MS, Vance ME, Farmer DK, Chan AWH, Abbatt JPD. 2024. Speciating volatile organic compounds in indoor air: Using in situ GC to interpret real-time PTR-MS signals. *Environmental Science: Processes & Impacts* (Royal Society of Chemistry). doi:10.1039/d4em00602j

Dixon JL, Beale R, Nightingale PD. 2013. Production of methanol, acetaldehyde, and acetone in the Atlantic Ocean. *Geophysical Research Letters* 40(17): 4700–4705. doi:10.1002/grl.50922

Dixon JL, Beale R, Sargeant SL, Tarran GA, Nightingale PD. 2014. Microbial acetone oxidation in coastal seawater. *Frontiers in Microbiology* 5: 243. doi:10.3389/fmicb.2014.00243

Dumont I, Schoemann V, Lannuzel D, Chou L, Tison J-L, Becquevort S. 2009. Distribution and characterization of dissolved and particulate organic matter in Antarctic pack ice. *Polar Biology* 32: 733–750. doi:10.1007/s00300-008-0577-y

Duprat L, Kanna N, Janssens J, Roukaerts A, Deman F, Townsend AT, Meiners KM, van der Merwe P, Lannuzel D. 2019. Enhanced iron flux to Antarctic sea ice via dust deposition from ice‐free coastal areas. *Journal of Geophysical Research: Oceans* 124: 8538–8557. doi:10.1029/2019jc015221

Edler L, Elbrächter M. 2010. The Utermöhl Method for Quantitative Phytoplankton Analysis. In: *Microscopic and Molecular Methods for Quantitative Phytoplankton Analysis*.

Engel A. 2009. Determination of marine gel particles. In: Wurl O (ed) *Practical Guidelines for the Analysis of Seawater*. CRC Press, p. 125–142.

Ferracci V, Weber J, Bolas CG, Robinson AD, Tummon F, Rodríguez‐Ros P, Cortés‐Greus P, Baccarini A, Jones RL, Galí M, Simó R, Schmale J, Harris NRP. 2024. Atmospheric isoprene measurements reveal larger‐than‐expected Southern Ocean emissions. *Nature Communications* 15: 2571. doi:10.1038/s41467-024-46744-4

Fiddes SL, Protat A, Mallet MD, Alexander SP, Woodhouse MT. 2022. Southern Ocean cloud and shortwave radiation biases in a nudged climate model simulation: does the model ever get it right? *Atmospheric Chemistry and Physics* 22: 14603–14630. doi:10.5194/acp-22-14603-2022

Fitzsimons MF, Airs R, Chen Y. 2024. The occurrence and biogeochemical cycling of quaternary, ternary and volatile amines in marine systems. *Frontiers in Marine Science* 11: 1466221. doi:10.3389/fmars.2024.1466221

Fitzsimons MF, Tilley M, Cree CHL. 2023. The determination of volatile amines in aquatic marine systems: A review. *Analytica Chimica Acta* 1241: 340707. doi:10.1016/j.aca.2022.340707

Fripiat F, Meiners KM, Vancoppenolle M, Papadimitriou S, Thomas DN, Ackley SF, Arrigo KR, Carnat G, Cozzi S, Delille B, Dieckmann GS, Dunbar RB, Fransson A, Kattner G, Kennedy H, Lannuzel D, Munro DR, Nomura D, Rintala J‐M, Schoemann V, Stefels J, Steiner N, Tison J‐L. 2017. Macro‐nutrient concentrations in Antarctic pack ice: Overall patterns and overlooked processes. *Elementa: Science of the Anthropocene* 5: 13. doi:10.1525/elementa.217

Fripiat F, Sigman DM, Fawcett SE, Rafter PA, Weigand MA, Tison J-L. 2014. New insights into sea ice nitrogen biogeochemical dynamics from the nitrogen isotopes. *Global Biogeochemical Cycles* 28: 115–130. doi:10.1002/2013gb004729

Fripiat F, Sigman DM, Massé G, Tison J-L. 2015. High turnover rates indicated by changes in the fixed N forms and their stable isotopes in Antarctic landfast sea ice. *Journal of Geophysical Research: Oceans* 120: 3079–3097. doi:10.1002/2014jc010583

Fung KM, Heald CL, Kroll JH, Wang S, Jo DS, Gettelman A, Lu Z, Liu X, Zaveri RA, Apel EC, Blake DR, Jimenez J-L, Campuzano-Jost P, Veres PR, Bates TS, Shilling JE, Zawadowicz M. 2022. Exploring dimethyl sulfide (DMS) oxidation and implications for global aerosol radiative forcing. *Atmospheric Chemistry and Physics* 22: 1549–1573. doi:10.5194/acp-22-1549-2022

Galí M, Devred E, Levasseur M, Royer S-J, Babin M. 2015. A remote sensing algorithm for planktonic dimethylsulfoniopropionate (DMSP) and an analysis of global patterns. *Remote Sensing of Environment* 171: 171–184. doi:10.1016/j.rse.2015.10.012

Garrison DL, Close AR. 1993. Winter ecology of the sea ice biota in Weddell Sea pack ice. *Marine Ecology Progress Series* 96: 17–31. doi:10.3354/meps096017

Gasol JM, Del Giorgio PA. 2000. Using flow cytometry for counting natural planktonic bacteria and understanding the structure of planktonic bacterial communities. *Scientia Marina* 64: 197–224. doi:10.3989/scimar.2000.64n2197

Golden KM. 2003. Critical behavior of transport in sea ice. *Physica B* 338: 274–283. doi:10.1016/j.physb.2003.08.007

Gowing MM, Garrison DL, Gibson AH, Krupp JM, Jeffries MO, Fritsen CH. 2004. Bacterial and viral abundance in Ross Sea summer pack ice communities. *Marine Ecology Progress Series* 279: 3–12. doi:10.3354/meps279003

Gradinger R, Ikävalko J. 1998. Organism incorporation into newly forming Arctic sea ice in the Greenland Sea. *Journal of Plankton Research* 20: 871–886. doi:10.1093/plankt/20.5.871

Gros V, Bonsang B, Sarda-Estève R, Nikolopoulos A, Metfies K, Wietz M, Peeken I. 2023. Concentrations of dissolved dimethyl sulfide (DMS), methanethiol and other trace gases in context of microbial communities from the temperate Atlantic to the Arctic Ocean. *Biogeosciences* 20: 851–867. doi:10.5194/bg-20-851-2023

Günther S, Gleitz M, Dieckmann GS. 1999. Biogeochemistry of Antarctic sea ice: a case study on platelet ice layers at Drescher Inlet, Weddell Sea. *Marine Ecology Progress Series* 177: 1–13. doi:10.3354/meps177001

Halsey KH, Giovannoni SJ, Graus M, Zhao Y, Landry Z, Thrash JC, Vergin KL, de Gouw J. 2017. Biological cycling of volatile organic carbon by phytoplankton and bacterioplankton. *Limnology and Oceanography* 62: 2650–2661. doi:10.1002/lno.10596

Heald CL, Goldstein AH, Allan JD, Aiken AC, Apel E, Atlas EL, Baker AK, Bates TS, Beyersdorf AJ, Blake DR, Campos T, Coe H, Crounse JD, DeCarlo PF, de Gouw JA, Dunlea EJ, Flocke FM, Fried A, Goldan P, Griffin RJ, Herndon SC, Holloway JS, Holzinger R, Jimenez JL, Junkermann W, Kuster WC, Lewis AC, Meinardi S, Millet DB, Onasch T, Polidori A, Quinn PK, Riemer DD, Roberts JM, Salcedo D, Sive B, Swanson AL, Talbot R, Warneke C, Weber RJ, Weibring P, Wennberg PO, Worsnop DR, Wittig AE, Zhang R, Zheng J & Zheng W. 2008. Total observed organic carbon (TOOC) in the atmosphere: a synthesis of North American observations. *Atmospheric Chemistry and Physics* 8: 2007–2025. doi:10.5194/acp-8-2007-2008

Hopkins FE, Archer SD, Bell TG, Suntharalingam P, Todd JD. 2023. The biogeochemistry of marine dimethylsulfide. *Nature Reviews Earth & Environment* 4: 361–376. doi:10.1038/s43017-023-00428-7

Howard EC, Henriksen JR, Buchan A, Reisch CR, Bürgmann H, Welsh R, Ye W, González JM, Mace K, Joye SB, Moran MA. 2006. Bacterial taxa that limit sulfur flux from the ocean. *Science* 314: 649–652. doi:10.1126/science.1130657

Jensen AR, Koss AR, Hales RB, de Gouw JA. 2023. Measurements of volatile organic compounds in ambient air by gas-chromatography and real-time Vocus PTR-TOF-MS: calibrations,

instrument background corrections, and introducing a PTR Data Toolkit. *Atmospheric Measurement Techniques* 16: 5261–5285. doi:10.5194/amt-16-5261-2023

Kattner G, Thomas DN, Haas C, Kennedy H, Dieckmann GS. 2004. Surface ice and gap layers in Antarctic sea ice: highly productive habitats. *Marine Ecology Progress Series* 277: 1–12. doi:10.3354/meps277001

Kettle AJ, Rhee TS, von Hobe M, Poulton A, Aiken J, Andreae MO. 2001. Assessing the flux of different volatile sulfur gases from the ocean to the atmosphere. *Journal of Geophysical Research: Atmospheres* 106(D11): 12193–12209. doi:10.1029/2000JD900630

Kiene RP. 1996. Production of methanethiol from dimethylsulfoniopropionate in marine surface waters. *Marine Chemistry* 54(1–2): 69–83. doi:10.1016/0304-4203(96)00006-0

Kiene RP, Dacey J, Rellinger AN, Williams TE. 2021. Standing stocks and rates for organic sulfur compounds during summer in the subarctic Northeast Pacific. *Biological and Chemical Oceanography Data Management Office (BCO-DMO)*. doi:10.26008/1912/BCO-DMO.705636.2

Kiene RP, Linn LJ, Bruton JA. 2000. New and important roles for DMSP in marine microbial communities. *Journal of Sea Research* 43(3–4): 209–224. doi:10.1016/s1385-1101(00)00023-x

Kinsey JD, Kieber DJ. 2016. Microwave preservation method for DMSP, DMSO, and acrylate in unfiltered seawater and phytoplankton culture samples. *Limnology and Oceanography: Methods* 14(3): 196–209. doi:10.1002/lom3.10081

Krembs C, Eicken H, Junge K, Deming JW. 2002. High concentrations of exopolymeric substances in Arctic winter sea ice: implications for the polar ocean carbon cycle and cryoprotection of diatoms. *Deep Sea Research Part I: Oceanographic Research Papers* 49(12): 2163–2181. doi:10.1016/s0967-0637(02)00122-x

Krembs C, Engel A. 2001. Abundance and variability of microorganisms and transparent exopolymer particles across the ice–water interface of melting first-year sea ice in the Laptev Sea (Arctic). *Marine Biology* 138(1): 173–185. doi:10.1007/s002270000396

Lannuzel D, Vancoppenolle M, van der Merwe P, de Jong J, Meiners KM, Grotti M, Nishioka J, Schoemann V. 2016. Iron in sea ice: Review and new insights. *Elementa: Science of the Anthropocene* 4: 000130. doi:10.12952/journal.elementa.000130

van Leeuwe MA, Fenton M, Davey E, Rintala J-M, Jones EM, Meredith MP, Stefels J. 2022. On the phenology and seeding potential of sea-ice microalgal species. *Elementa: Science of the Anthropocene* 10(1). doi:10.1525/elementa.2021.00029

van Leeuwe MA, Tedesco L, Arrigo KR, Assmy P, Campbell K, Meiners KM, Rintala J-M, Selz V, Thomas DN, Stefels J. 2018. Microalgal community structure and primary production in Arctic and Antarctic sea ice: A synthesis. *Elementa: Science of the Anthropocene* 6(1): 4. doi:10.1525/elementa.267

Legendre L, Aota M, Shirasawa K, Martineau M-J, Ishikawa M. 1991. Crystallographic structure of sea ice along a salinity gradient and environmental control of microalgae in the brine cells. *Journal of Marine Systems* 2(3–4): 347–357. doi:10.1016/0924-7963(91)90041-r

Lemfack MC, Gohlke B-O, Toguem SMT, Preissner S, Piechulla B, Preissner R. 2018. mVOC 2.0: a database of microbial volatiles. *Nucleic Acids Research* 46(D1): D1261–D1265. doi:10.1093/nar/gkx1016

Li C-X, Chen K, Sun X, Liu L, Xin M, Liu X-L, Wang B-D. 2024. Summer sea ice melting enhances phytoplankton and dimethyl sulfide production. *Limnology and Oceanography* 69(10): 2453–2472. doi:10.1002/lno.12681

Lidbury I, Mausz MA, Scanlan DJ, Chen Y. 2017. Identification of dimethylamine monooxygenase in marine bacteria reveals a metabolic bottleneck in the methylated amine degradation pathway. *ISME Journal* 11(7): 1592–1601. doi:10.1038/ismej.2017.31

Lim SM, Campbell K, Arrigo KR. in press 2025. Primary production associated with sea ice. In: Thomas DN, editor. *Sea Ice 4th Edition – Its Physics, Chemistry, Biology, Geology and Societal Importance*. Oxford: Wiley.

Liu C, Li H, Zheng H, Wang G, Qin X, Chen J, Zhou S, Lu D, Liang G, Song X, Duan Y, Liu J, Huang K, Deng C. 2022. Ocean emission pathway and secondary formation mechanism of

aminiums over the Chinese marginal sea. *Journal of Geophysical Research: Atmospheres* 127: e2022JD037805. doi:10.1029/2022JD037805

Luhtanen A-M, Eronen-Rasimus E, Oksanen HM, Tison J-L, Delille B, Dieckmann GS, Rintala J-M. 2018. The first known virus isolates from Antarctic sea ice have complex infection patterns. *FEMS Microbiology Ecology* 94(4): fiy028. doi:10.1093/femsec/fiy028

Lund-Hansen LC, Gradinger R, Hassett B, Jayasinghe S, Kennedy F, Martin A, McMinn A, Søgaard DH, Sorrell BK. 2024. Sea ice as habitat for microalgae, bacteria, virus, fungi, meio- and macrofauna: A review of an extreme environment. *Polar Biology*. in press. doi:10.1007/s00300-024-03296-z

Malinverno E, Maffioli P, Gariboldi K. 2016. Latitudinal distribution of extant fossilizable phytoplankton in the Southern Ocean: Planktonic provinces, hydrographic fronts and palaeoecological perspectives. *Marine Micropaleontology* 123:41–58. doi:10.1016/j.marmicro.2016.01.001

Mallet MD, Humphries RS, Fiddes SL, Alexander SP, Altieri K, Angot H, Anilkumar N, Bartels‐Rausch T, Creamean J, Dall'Osto M, Dommergue A, Frey M, Henning S, Lannuzel D, Lapere R, Mace GG, Mahajan AS, McFarquhar GM, Meiners KM, Miljevic B, Peeken I, Protat A, Schmale J, Steiner N, Sellegri K, Simó R, Thomas J‐L, Willis MD, Winton VHL & Woodhouse MT. 2023. Untangling the influence of Antarctic and Southern Ocean life on clouds. *Elementa: Science of the Anthropocene* 11(1): 00130. doi:10.1525/elementa.2022.00130

Maranger R, Bird DR, Juniper SK. 1994. Viral and bacterial dynamics in Arctic sea ice during the spring algal bloom near Resolute, N.W.T., Canada. *Marine Ecology Progress Series* 111:121–127. doi:10.3354/meps111121

Masdeu-Navarro M, Mangot J-F, Xue L, Cabrera-Brufau M, Gardner SG, Kieber DJ, González JM. 2022. Spatial and diel patterns of volatile organic compounds, DMSP-derived compounds, and planktonic microorganisms around a tropical scleractinian coral colony. *Frontiers in Marine Science* 9:944141. doi:10.3389/fmars.2022.944141

Mausz MA, Chen Y. 2019. Microbiology and ecology of methylated amine metabolism in marine ecosystems. *Current Issues in Molecular Biology* 33:133–148. doi:10.21775/cimb.033.133

McCoy DT, Burrows SM, Wood R, Grosvenor DP, Elliott SM, Ma P-L, Rasch PJ, Hartmann DL. 2015. Natural aerosols explain seasonal and spatial patterns of Southern Ocean cloud albedo. *Science Advances* 1(6):e1500157. doi:10.1126/sciadv.1500157

Meiners K, Brinkmeyer R, Granskog MA, Lindfors A. 2004. Abundance, size distribution and bacterial colonization of exopolymer particles in Antarctic sea ice (Bellingshausen Sea). *Aquatic Microbial Ecology* 35:283–296. doi:10.3354/ame035283

Meiners KM, Vancoppenolle M, Carnat G, Castellani G, Delille B, Delille D, Dieckmann GS, Flores H, Fripiat F, Grotti M, Ackley SF, Arrigo KR, Thomas DN. 2018. Chlorophyll‐a in Antarctic landfast sea ice: A first synthesis of historical ice core data. *Journal of Geophysical Research: Oceans* 123(11):8444–8459. doi:10.1029/2018jc014245

Meiners KM, Vancoppenolle M, Thanassekos S, Dieckmann GS, Thomas DN, Tison J-L, Arrigo KR, Garrison DL, McMinn A, Lannuzel D, Campbell K, Ackley SF. 2012. Chlorophyll in Antarctic sea ice from historical ice core data. *Geophysical Research Letters* 39(21): L21602. doi:10.1029/2012gl053478

Miller LA, Fripiat F, Else BGT, Bowman JS, Brown KA, Collins RE, Ewert M, Fransson A, Gosselin M, Lannuzel D, Meiners KM, Papakyriakou T, Rintala J-M, Tison J-L, Thomas DN, Vancoppenolle M, Vernet M. 2015. Methods for biogeochemical studies of sea ice: The state of the art, caveats, and recommendations. *Elementa: Science of the Anthropocene* 3: 000038. doi:10.12952/journal.elementa.000038

Misztal PK, Hewitt CN, Wildt J, Blande JD, Eller AS‐D, Fares S, Gentner DR, Gilman JB, Graus M, Greenberg J, Guenther AB, Hansel A, Harley P, Huang M, Jardine K, Karl T, Kaser L, Keutsch FN, Kiendler‐Scharr A, Kleist E, Lerner BM, Li T, Mak J, Nölscher AC, Schnitzhofer R, Sinha V, Thornton B, Warneke C, Wegener F, Werner C, Williams J, Worton DR, Yassaa N & Goldstein AH. 2015. Atmospheric benzenoid emissions from plants rival those from fossil fuels. *Scientific Reports* 5: 12064. doi:10.1038/srep12064

Montresor M, Procaccini G, Stoecker DK. 1999. *Polarella glacialis*, gen. nov., sp. nov. (Dinophyceae): Suessiaceae are still alive! *Journal of Phycology* 35(1): 186–197. doi:10.1111/j.0022-3646.1999.00186.x

Montresor M, Procaccini G, Stoecker DK. 1999. *Polarella glacialis*, gen. nov., sp. nov. (Dinophyceae): Suessiaceae are still alive! *Journal of Phycology* 35(1): 186–197. doi:10.1111/j.0022-3646.1999.00186.x

Moran MA, Reisch CR, Kiene RP, Whitman WB. 2012. Genomic insights into bacterial DMSP transformations. *Annual Review of Marine Science* 4: 523–542. doi:10.1146/annurev-marine-120710-100827

Mynard C, Franklin EB, Alroe J, Somerville N, Patti A, Siems ST, Williams AG, Mallet M, Humphries RS, Dunne E. 2025. Constraining atmospheric methanethiol estimates over the Southern Ocean. *ESS Open Archive*. doi:10.22541/essoar.174595010.02620308/v2

Nomura D, Koga S, Kasamatsu N, Shinagawa H, Simizu D, Wada M, Fukuchi M. 2012. Direct measurements of DMS flux from Antarctic fast sea ice to the atmosphere by a chamber technique. *Journal of Geophysical Research: Oceans* 117(C4). doi:10.1029/2010JC006755

Notz D, Worster MG. 2009. Desalination processes of sea ice revisited. *Journal of Geophysical Research: Oceans* 114(C5). doi:10.1029/2008JC004885

Omori Y, Takahashi T, Wada S, Hama T, Inomata S, Tanimoto H. 2025. Production of oxygen- and sulfur-containing volatile organic compounds by marine bacteria from coastal seawater. *Journal of Geophysical Research: Biogeosciences* 130(10). doi:10.1029/2025JG008969

Padaki VG, Palmer E, Jiang Y, Buchholz HH, Kimbrel JA, Halsey KH. 2025. Diatom volatile organic compound production is driven by diel metabolism and the cell cycle. *Frontiers in Microbiology* 16:1620542. doi:10.3389/fmicb.2025.1620542

Pfannerstill EY, Arata C, Zhu Q, Schulze BC, Ward R, Woods R, Harkins C, Schwantes RH, Seinfeld JH, Bucholtz A, Cohen RC, Goldstein AH. 2024. Temperature-dependent emissions dominate aerosol and ozone formation in Los Angeles. *Science* 384(6702):1324–1329. doi:10.1126/science.adg8204

van Pinxteren M, Fomba KW, van Pinxteren D, Triesch N, Hoffmann EH, Cree CHL, Fitzsimons MF, von Tümpling W, Herrmann H. 2019. Aliphatic amines at the Cape Verde Atmospheric Observatory: Abundance, origins and sea-air fluxes. *Atmospheric Environment* 203:183–195. doi:10.1016/j.atmosenv.2019.02.011

Piquet AM-T, Bolhuis H, Davidson AT, Thomson PG, Buma AGJ. 2008. Diversity and dynamics of Antarctic marine microbial eukaryotes under manipulated environmental UV radiation. *FEMS Microbiology Ecology* 66(2):352–366. doi:10.1111/j.1574-6941.2008.00588.x

Petrich C, Eicken H. 2010. Growth, structure and properties of sea ice. In: Thomas DN, Dieckmann GS, editors. *Sea Ice*, 2nd edition. Oxford: Wiley-Blackwell. p. 23–77.

Reisch CR, Stoudemayer MJ, Varaljay VA, Amster IJ, Moran MA, Whitman WB. 2011. Novel pathway for assimilation of dimethylsulphoniopropionate widespread in marine bacteria. *Nature* 473(7346): 208–211. doi:10.1038/nature10078

Rellinger AN, Kiene RP, del Valle DA, Kieber DJ, Slezak D, Harada H, Bisgrove J, Brinkley J. 2009. Occurrence and turnover of DMSP and DMS in deep waters of the Ross Sea, Antarctica. *Deep Sea Research Part I: Oceanographic Research Papers* 56(5): 686–702. doi:10.1016/j.dsr.2008.12.010

Riaux-Gobin C, Stumm K. 2006. Modern Archaeomonadaceae from the land-fast ice off Adélie Land, East Antarctica: a preliminary report. *Antarctic Science* 18(1): 51–60. doi:10.1017/s0954102006000046

Riedel A, Michel C, Gosselin M, LeBlanc B. 2007. Enrichment of nutrients, exopolymeric substances and microorganisms in newly formed sea ice on the Mackenzie shelf. *Marine Ecology Progress Series* 342: 55–67. doi:10.3354/meps342055

Riedel A, Michel C, Gosselin M, LeBlanc B. 2008. Winter–spring dynamics in sea-ice carbon cycling in the coastal Arctic Ocean. *Journal of Marine Systems* 74(3–4): 918–932. doi:10.1016/j.jmarsys.2008.01.003

Rinaldi M, Paglione M, Decesari S, Harrison RM, Beddows DCS, Ovadnevaite J, Ceburnis D, O'Dowd CD, Simó R, Dall'Osto M. 2020. Contribution of water-soluble organic matter from

multiple marine geographic eco-regions to aerosols around Antarctica. *Environmental Science & Technology* 54(13): 7807–7817. doi:10.1021/acs.est.0c00695

Rocchi A, Fitzsimons MF, Akenga P, Sotomayor A, Sà EL, Güell-Bujons Q, Vila M, Castillo YM, Dall'Osto M, Vaqué D, Wohl C, Simó R, Berdalet E. 2025. Distribution of alkylamines in surface waters around the Antarctic Peninsula and Weddell Sea. doi: 10.5194/egusphere-2025-407

Rocchi A, Sotomayor-Garcia A, Cabrera-Brufau M, Berdalet E, Dall'Osto M, Vaqué D. 2022. Abundance and activity of sympagic viruses near the Western Antarctic Peninsula. *Polar Biology* 45(8): 1363–1378. doi:10.1007/s00300-022-03073-w

Rocco M, Dunne E, Peltola M, Barr N, Williams J, Colomb A, Safi K, Saint-Macary A, Marriner A, Deppeler S, Harnwell J, Law C, Sellegri K. 2021. Oceanic phytoplankton are a potentially important source of benzenoids to the remote marine atmosphere. *Communications Earth & Environment* 2(1). doi:10.1038/s43247-021-00253-0

Rodríguez-Ros P, Galí M, Cortés P, Robinson CM, Antoine D, Wohl C, Yang M, Simó R. 2020. Remote sensing retrieval of isoprene concentrations in the Southern Ocean. *Geophysical Research Letters* 47(13). doi:10.1029/2020GL087888

Romoli, R., Papaleo, M. C., de Pascale, D., Tutino, M. L., Michaud, L., LoGiudice, A., Fani, R., Bartolucci, G. 2011. Characterization of the volatile profile of Antarctic bacteria by using solid-phase microextraction-gas chromatography-mass spectrometry. Journal of Mass Spectrometry 46(10): 1051–1059. doi:10.1002/jms.1987

Roukaerts A, Deman F, Van der Linden F, Carnat G, Bratkic A, Moreau S, Lannuzel D, Dehairs F, Delille B, Tison J-L, Fripiat F. 2021. The biogeochemical role of a microbial biofilm in sea ice: Antarctic landfast sea ice as a case study. *Elementa: Science of the Anthropocene* 9(1): 00134. doi:10.1525/elementa.2020.00134

Sander R. 2023. Compilation of Henry's law constants (version 5.0.0) for water as solvent. *Atmospheric Chemistry and Physics* 23(19): 10901–12440. doi:10.5194/acp-23-10901-2023

Schlundt C, Tegtmeier S, Lennartz ST, Bracher A, Cheah W, Krüger K, Quack B, Marandino CA. 2017. Oxygenated volatile organic carbon in the western Pacific convective center: ocean

cycling, air–sea gas exchange and atmospheric transport. *Atmospheric Chemistry and Physics* 17(17): 10837–10854. doi:10.5194/acp-17-10837-2017

Shaw SL, Gantt B, Meskhidze N. 2010. Production and emissions of marine isoprene and monoterpenes: A review. *Advances in Meteorology* 2010(1): 1–24. doi:10.1155/2010/408696

Simó R. 2001. Production of atmospheric sulfur by oceanic plankton: biogeochemical, ecological and evolutionary links. *Trends in Ecology & Evolution* 16(6): 287–294. doi:10.1016/s0169-5347(01)02152-8

Simó R, Cortés-Greus P, Rodríguez-Ros P, Masdeu-Navarro M. 2022. Substantial loss of isoprene in the surface ocean due to chemical and biological consumption. *Communications Earth & Environment* 3(1). doi:10.1038/s43247-022-00352-6

Staudinger J, Roberts PV. 2001. A critical compilation of Henry's law constant temperature dependence relations for organic compounds in dilute aqueous solutions. *Chemosphere* 44(4):561–576. doi:10.1016/s0045-6535(00)00505-1

Stefels J, Carnat G, Dacey JWH, Goossens T, Elzenga JTM, Tison J-L. 2012. The analysis of dimethylsulfide and dimethylsulfoniopropionate in sea ice: Dry-crushing and melting using stable isotope additions. *Marine Chemistry* 128–129:34–43. doi:10.1016/j.marchem.2011.09.007

Stefels J, van Leeuwe MA, Jones EM, Meredith MP, Venables HJ, Webb AL, Henley SF. 2018. Impact of sea-ice melt on dimethyl sulfide (sulfoniopropionate) inventories in surface waters of Marguerite Bay, West Antarctic Peninsula. *Philosophical Transactions of the Royal Society A: Mathematical, Physical and Engineering Sciences* 376(2122). doi:10.1098/rsta.2017.0169

Stefels J, Steinke M, Turner S, Malin G, Belviso S. 2007. Environmental constraints on the production and removal of the climatically active gas dimethylsulphide (DMS) and implications for ecosystem modelling. *Biogeochemistry* 83(1–3):245–275. doi:10.1007/s10533-007-9091-5

Stein LY. 2017. Methylamine: a vital nitrogen (and carbon) source for marine microbes. *Environmental Microbiology* 19(6):2117–2118. doi:10.1111/1462-2920.13716

Stoecker DK, Li A, Coats DW, Gustafson DE, Nannen MK. 1997. Mixotrophy in the dinoflagellate *Prorocentrum minimum*. *Marine Ecology Progress Series* 152:1–12. doi:10.3354/meps152001

Taubert M, Grob C, Howat AM, Burns OJ, Pratscher J, Jehmlich N, von Bergen M, Richnow HH, Chen Y, Murrell JC. 2017. Methylamine as a nitrogen source for microorganisms from a coastal marine environment. *Environmental Microbiology* 19(6):2246–2257. doi:10.1111/1462-2920.13709

Teng Z-J, Qin Q-L, Zhang W, Li J, Fu H-H, Wang P, Lan M, Luo G, He J, McMinn A, Wang M, Chen X-L, Zhang Y-Z, Chen Y, Li C-Y. 2021. Biogeographic traits of dimethyl sulfide and dimethylsulfoniopropionate cycling in polar oceans. *Microbiome* 9: 207. doi:10.1186/s40168-021-01153-3

Thomas DN, Dieckmann GS. 2002. Antarctic sea ice—a habitat for extremophiles. *Science* 295: 641–644. doi:10.1126/science.1063391

Thomas DN, Papadimitriou S, Michel C. 2010. Biogeochemistry of sea ice. In: Thomas DN, Dieckmann GS, editors. *Sea Ice*. Oxford (UK): Blackwell Science.

Thomas DN, Kattner G, Engbrodt R, Giannelli V, Kennedy H, Haas C, Dieckmann GS. 2001. Dissolved organic matter in Antarctic sea ice. *Annals of Glaciology* 33: 297–303. doi:10.3189/172756401781818338

Tison J-L, Brabant F, Dumont I, Stefels J. 2010. High-resolution dimethyl sulfide and dimethylsulfoniopropionate time series profiles in decaying summer first-year sea ice at Ice Station Polarstern, western Weddell Sea, Antarctica. *Journal of Geophysical Research: Oceans* 115(G4). doi:10.1029/2010JG001427

Torstensson A, Dinasquet J, Chierici M, Fransson A, Riemann L, Wulff A. 2015. Physicochemical control of bacterial and protist community composition and diversity in Antarctic sea ice. *Environmental Microbiology* 17(10): 3869–3881. doi:10.1111/1462-2920.12865

Trevena AJ, Jones GB. 2006. Dimethylsulphide and dimethylsulphoniopropionate in Antarctic sea ice and their release during sea ice melting. *Marine Chemistry* 98(2–4): 210–222. doi:10.1016/j.marchem.2005.09.005

Trevena AJ, Jones GB, Wright SW, van den Enden RL. 2003. Profiles of dimethylsulphoniopropionate (DMSP), algal pigments, nutrients, and salinity in the fast ice of Prydz Bay, Antarctica. *Journal of Geophysical Research: Oceans* 108(C5). doi:10.1029/2002JC001369

Underwood GJC, Fietz S, Papadimitriou S, Thomas DN, Dieckmann GS. 2010. Distribution and composition of dissolved extracellular polymeric substances (EPS) in Antarctic sea ice. *Marine Ecology Progress Series* 404:1–19. doi:10.3354/meps08557

Vancoppenolle M, Meiners KM, Michel C, Bopp L, Brabant F, Carnat G, Delille B, Lannuzel D, Madec G, Moreau S, Tison J-L, Arrigo KR, Thomas DN, Papadimitriou S. 2013. Role of sea ice in global biogeochemical cycles: emerging views and challenges. *Quaternary Science Reviews* 79:207–230. doi:10.1016/j.quascirev.2013.04.011

Van der Linden FC, Tison J-L, Champenois W, Moreau S, Carnat G, Kotovitch M, Fripiat F, Deman F, Roukaerts A, Dehairs F, Thomas DN, Vancoppenolle M, Lannuzel D, Arrigo KR, Meiners KM, Papadimitriou S. 2020. Sea ice CO2 dynamics across seasons: impact of processes at the interfaces. *Journal of Geophysical Research: Oceans* 125(6). doi:10.1029/2019JC015807

Vaqué D, Boras JA, Arrieta JM, Agustí S, Duarte CM, Sala MM. 2021. Enhanced viral activity in the surface microlayer of the Arctic and Antarctic oceans. *Microorganisms* 9(2):317. doi:10.3390/microorganisms9020317

Vaulot D, Courties C, Partensky F. 1989. A simple method to preserve oceanic phytoplankton for flow cytometric analyses. *Cytometry* 10(5):629–635. doi:10.1002/cyto.990100519

Wang N, Chen X-L, Gao C, Peng M, Wang P, Zhang N, Li F, Yang G-P, Shen Q-T, Li S, Chen Y, Zhang Y-Z, Li C-Y. 2021. Crystal structures of γ-glutamylmethylamide synthetase provide insight into bacterial metabolism of oceanic monomethylamine. *Journal of Biological Chemistry* 296: 100081. doi:10.1074/jbc.RA120.015952

Wilkins D, Yau S, Williams TJ, Allen MA, Brown MV, DeMaere MZ, Lauro FM, Cavicchioli R. 2013. Key microbial drivers in Antarctic aquatic environments. *FEMS Microbiology Reviews* 37(3): 303–335. doi:10.1111/1574-6976.12007

Willis MD, Lannuzel D, Else B, Angot H, Campbell K, Crabeck O, Delille B, Hayashida H, Lizotte M, Loose B, Meiners KM, Miller L, Moreau S, Nomura D, Prytherch J, Schmale J, Steiner N, Tedesco L, Thomas J. 2023. Polar oceans and sea ice in a changing climate. *Elementa: Science of the Anthropocene* 11(1): 00056. doi:10.1525/elementa.2023.00056

Wohl C, Brown I, Kitidis V, Jones AE, Sturges WT, Nightingale PD, Yang M. 2020. Underway seawater and atmospheric measurements of volatile organic compounds in the Southern Ocean. *Biogeosciences* 17(9): 2593–2619. doi:10.5194/bg-17-2593-2020

Wohl C, Capelle D, Jones A, Sturges WT, Nightingale PD, Else BGT, Yang M. 2019. Segmented flow coil equilibrator coupled to a proton-transfer-reaction mass spectrometer for measurements of a broad range of volatile organic compounds in seawater. *Ocean Science* 15(4): 925–940. doi:10.5194/os-15-925-2019

Wohl C, Güell-Bujons Q, Castillo YM, Calbet A, Simó R. 2023a. Volatile organic compounds released by *Oxyrrhis marina* grazing on *Isochrysis galbana*. *Oceans* 4(2): 151–169. doi:10.3390/oceans4020011

Wohl C, Jones AE, Sturges WT, Nightingale PD, Else B, Butterworth BJ, Yang M. 2022. Sea ice concentration impacts dissolved organic gases in the Canadian Arctic. *Biogeosciences* 19(4): 1021–1045. doi:10.5194/bg-19-1021-2022

Wohl C, Li Q, Cuevas CA, Fernandez RP, Yang M, Saiz-Lopez A, Simó R. 2023b. Marine biogenic emissions of benzene and toluene and their contribution to secondary organic aerosols over the polar oceans. *Science Advances* 9(4): eadd9031. doi:10.1126/sciadv.add9031

Wohl C, Villamayor J, Galí M, Mahajan AS, Fernández RP, Cuevas CA, Bossolasco A, Li Q, Kettle AJ, Williams T, Simoneit BRT, Wang P, Rinaldi M, Dall'Osto M, Vaqué D, Simó R. 2024. Marine emissions of methanethiol increase aerosol cooling in the Southern Ocean. *Science Advances* 10(48): eadq2465. doi:10.1126/sciadv.adq2465

Yentsch CS, Menzel DW. 1963. A method for the determination of phytoplankton chlorophyll and phaeophytin by fluorescence. *Deep Sea Research and Oceanographic Abstracts* 10(3): 221–231. doi:10.1016/0011-7471(63)90358-9

Zemmelink HJ, Dacey JWH, Houghton L, Hintsa EJ, Liss PS. 2008. Dimethylsulfide emissions over the multi-year ice of the western Weddell Sea. *Geophysical Research Letters* 35(6). doi:10.1029/2007gl031847

Zemmelink HJ, Houghton L, Dacey JWH, Worby AP, Liss PS. 2005. Emission of dimethylsulfide from Weddell Sea leads. *Geophysical Research Letters* 32(23). doi:10.1029/2005GL024242

Zemmelink HJ, Houghton L, Frew NM, Dacey JWH. 2006. Dimethylsulfide and major sulfur compounds in a stratified coastal salt pond. *Limnology and Oceanography* 51(1): 271–279. doi:10.4319/lo.2006.51.1.0271

Zhou J, Delille B, Eicken H, Vancoppenolle M, Brabant F, Carnat G, Geilfus N-X, Papakyriakou T, Heinesch B, Tison J-L. 2013. Physical and biogeochemical properties in landfast sea ice (Barrow, Alaska): Insights on brine and gas dynamics across seasons. *Journal of Geophysical Research: Oceans* 118(6): 3172–3189. doi:10.1002/jgrc.20232

Zhou L, Booge D, Zhang M, Marandino CA. 2022. Winter season Southern Ocean distributions of climate-relevant trace gases. *Biogeosciences* 19(20): 5021–5040. doi:10.5194/bg-19-5021-2022

Zhu Y, Kieber DJ. 2018. Wavelength- and temperature-dependent apparent quantum yields for photochemical production of carbonyl compounds in the North Pacific Ocean. *Environmental Science & Technology* 52(4): 1929–1939. doi:10.1021/acs.est.7b05462

Figure caption

Figure 1. Sea ice physical properties. Temperature in (°C) and brine volume fraction (%) profiles in the sea ice cores **(A)**. IQR box plots of the salinity **(B)** and enrichment factor (%) **(C)** for the top (n = 5), middle (Mid, n = 6) and bottom (Bot, n = 5) ice layers, brine (n = 12) and seawater (n = 5). Box plots show the interquartile range (IQR; 25th–75th percentile), with the horizontal line indicating the median and whiskers extending to 1.5 × IQR.

Figure 2. Biological properties of the sea ice, brines and seawater. IQR box plot of the concentration and enrichment factor of the following parameters: Chl-a **(A and C)**, POC **(B and C)**, PON **(B and C)**; virus **(D and F)** and bacterial (**E and F)**, TEP **(G)**, for the top, middle (Mid) and bottom (Bot) ice layers, brine and seawater. The abundances of the main microplankton groups (diatoms, dinoflagellates and ciliates) expressed as % of the total cell numbers in **(K)**. Box plots show the interquartile range (IQR; 25th–75th percentile), with the horizontal line indicating the median and whiskers extending to 1.5 × IQR. The number of data points for each box plot is reported in Table 1.

Figure 3. Nutrient concentrations in sea ice, brine and seawater. IQR Box plot of the concentration and enrichment factor of Nitrate plus nitrite **(A and E)**, silicate **(B and E)**, Phosphate **(C and E)** and ammonium **(D and E)** for the top, middle (Mid) and bottom (Bot) ice layers, brine and seawater. Box plots show the interquartile range (IQR; 25th–75th percentile), with the horizontal line indicating the median and whiskers extending to 1.5 × IQR. The number of data points is reported in Table 1.

Figure 4. Alkylamines distribution in sea ice brine and seawater. IQR Box plots of total (particulate + dissolved) alkylamine concentrations (pTMA, dTMA, dDMA, dDEA) **(A)** and their enrichment factors **(B)**, along with the average relative abundance of each alkylamine with respect to the total **(C)** in the top (n = 3) and bottom (Bot, n = 3) ice layers, brine (n=8) and seawater (note that for alkylamine there were no middle-ice samples). Box plots show the interquartile range (IQR; 25th–75th percentile), with the horizontal line indicating the median and whiskers extending to 1.5 × IQR.

Figure 5. Sulfur compounds in sea ice, brine and seawater. IQR Box plots of MeSH (**A**), DMS (**B**), and DMSP (**C**) concentrations (nM) and their enrichment factors (%, **D**) in top (n = 6), middle (Mid, n = 5), and bottom (Bot, n = 5) ice layers, brine (n = 14) and seawater (n = 5). Along with the relationships between MeSH and DMS (**E**) and the ratio between MeSH:DMS (**F**). Box plots show

the interquartile range (IQR; 25th–75th percentile), with the horizontal line indicating the median and whiskers extending to 1.5 × IQR.

Figure 6.VOCs distribution in sea ice, brine and seawater. IQR Box plots of the concentrations (nM) of VOCs (Acetone, **A**; Isoprene, **B**; Benzene, **D**; Toluene, **E**; and Xylene, **F**) and their enrichment factors, % (**C**) in top (n = 6), middle (Mid, n = 5), and bottom (Bot, n = 5) ice layers, brine (n = 14) and seawater (n = 5). Box plots show the interquartile range (IQR; 25th–75th percentile), with the horizontal line indicating the median and whiskers extending to 1.5 × IQR.

Table Caption

Table 1. Biological and biogeochemical variables in sea ice, brine and seawater Columns depict the average ± standard deviation, the median and 25th-75th percentiles (IQR) of the concentrations or abundances, and the sample number (n) in top, middle (Mid) and bottom (Bot) layers of sea ice, as well as in brines and seawater (SW).

Table 2. Concentration of alkylamines, S-compounds and VOCs in sea ice, brine and seawater. The average ± standard deviation, the median concentrations, 25th and 75th percentile (IQR), and "n" sample number of key compounds (alkylamines, S-compounds and VOCs) in top, middle (Mid) and bottom (Bot) layers of sea ice, brines and seawater (SW) (na: not available).